2013

Ex vivo reprogramming of tumor-reactive immune cells from FVBN202 mice bearing lung metastatic mammary carcinoma: an immunotherapeutic opportunity revealed against recurrence

Charles Hall
Virginia Commonwealth University

Ex vivo reprogramming of tumor-reactive immune cells from FVBN202 mice bearing lung metastatic mammary carcinoma: an immunotherapeutic opportunity revealed against recurrence

A thesis submitted in partial fulfillment of the requirements for the degree of Master of Science at Virginia Commonwealth University.

by

Charles Edward Hall
Bachelor of Science, Biology
Bachelor of Music, Music Industry
James Madison University 2008

Director: Masoud Manjili, DVM, PhD
Associate Professor
Department of Microbiology and Immunology

Virginia Commonwealth University
Richmond, Virginia
August 1st, 2013

Acknowledgement

The author wishes to thank several people. I wish to thank my family that supported me during my time at VCU. My parents and sister have provided me with a great deal of patience while completing this project. My friends and Manjili labmates have also been supportive the last two years during all the long hours. In addition, I would like to thank Dr. Manjili for his direction, patience and mentorship with this extensive project. Finally, I dedicate my thesis work to my late grandfather, Charles Walker Hall, Jr., a prostate cancer survivor and long-time skin cancer sufferer. He was always supportive of my advanced studies in cancer research and passed away during my tenure at VCU. All of my family members that experienced cancer have been a great source of continuous inspiration.

Table of Contents

List of Tables

List of Figures

List of Abbreviations

Abs:	Antibodies, pertaining to flow cytometry staining of certain epitope signatures
ACK:	Ammonium-Chloride-Potassium lysing buffer for erythrocyte removal
ACT:	Adoptive cellular therapy
AICD:	Activation-induced cell death, results from T cell engagement with tumor
ANV:	Antigen-negative variant form of MMC with neu oncoprotein loss, cell line
B/I + IL-2:	Bryostatin 1/ Ionomycin + Interleukin-2 at Day 0, initiates reprogramming
B/I + γ-c:	Bryostatin 1/ Ionomycin + γ-chain cytokines (IL-2, IL-7, IL-15), for expansion
DCIS:	Ductal carcinoma in situ, early slow growing form of mammary cancer
DMSO:	Dimethyl Sulfoxide, prevents crystal formation upon freezing for cell viability
EDTA:	Ethylenediaminetetraacetic acid, chelating agent for gentle adherent cell removal
EMT:	Epithelial to mesenchymal transition
ER:	Estrogen receptor
FBS:	Fetal bovine serum, growth supplement
FITC:	Fluorescein isothiocyanate, fluorochrome used with 488 nm-wavelength laser
FVBN202:	Transgenic mouse model with an additional copy of rat neu oncoprotein inserted downstream of the MMTV promoter, resulting in neu overexpression
GVHD:	Graft versus host disease; donor-mismatch issue in recipients resulting in illness
HBSS:	Hank's balanced salt solution; salt solution with glucose added for cell stability
HER2/neu:	Human epidermal growth factor receptor 2/ neu oncoprotein

HPV: Human Papillomavirus; 100% effective prophylactic HPV vaccines produced

IACUC: Institutional animal care and use committee, VCU organization

i.v.: Intravenous, injection or treatment delivery

mANV: Metastatic antigen-negative variant of MMC, established tumor cells in culture

MCP-1/CCL2: Monocyte chemotactic protein 1 or chemokine (C-C motif) ligand 2, monocyte/macrophage macrophage chemoattractant associated with MMC

MDSC: Myeloid-derived suppressor cells, CDllb+ GR-1+

MET: Mesenchymal to epithelial transition

MMC: Mouse mammary carcinoma (neu-overexpressing), cell line

mMMC: Metastatic mouse mammary carcinoma, established tumor cells in culture

MMP/MMP9: Matrix metalloprotease; Matrix metalloprotease 9, TAM secreted and found in lung prior to metastasis

MMTV: Mouse mammary tumor virus

MTT: 3-(4,5-dimethylthiazol-2-yl)-2,5-diphenyltetrazolium bromide, indicator reagent

NK/NKT: Natural killer (CD3-CD49b+) or natural killer T cells (CD3+ CD49b+)

n.s.: Not significant, statistically; $p > 0.05$

PBS: Phosphate buffered saline solution (1X), washing solution

PE: Phycoerythrin, fluorochrome (488 laser)

PE/Cy5: Phycoerythrin conjugated to Cy5 molecule, fluorochrome (488 laser)

PI: Propidium iodide, used in viability studies to bind DNA indicating necrosis

PR: Progesterone receptor

s.c.: Subcutaneously tumor-challenged mice

SEM: Standard error of the mean

T_N: Naïve (N) T cells, CD44-CD62L+

T_{EM}: Effector memory (EM) T cells, CD44+CD62L+(low)

T_{CM}: Central memory (CM) T cells, CD44+CD62L+(high)

T_E: Effector (E) T cells, CD44+CD62L-

TAM: Tumor-associated macrophages, also known as M2 macrophages, Th2-skewed

TGF-β1: Transforming growth factor – beta, isoform 1; dual function cytokine for tumor

TME: Tumor microenvironment

VEGF: Vascular endothelial growth factor, angiogenic soluble factor

VEGFR1+: Vascular endothelial growth factor receptor 1 on endothelial cells, met. promoter

Abstract

EX VIVO REPROGRAMMING OF TUMOR-REACTIVE IMMUNE CELLS FROM FVBN202 MICE BEARING LUNG METASTATIC MAMMARY CARCINOMA: AN IMMUNOTHERAPEUTIC OPPORTUNITY REVEALED AGAINST RECURRENCE

By Charles Edward Hall, M.S.

A thesis submitted in partial fulfillment of the requirements for the degree of Master of Science at Virginia Commonwealth University.

Virginia Commonwealth University, 2013

Director: Masoud Manjili, DVM, PhD, Associate Professor,
Department of Microbiology and Immunology

Metastatic breast cancer treatment has seen few advances in recent years, yet treatment resistance continues to rise, causing disease recurrence. A pilot study was performed to determine the efficacy of *ex vivo* expansion and reprogramming of tumor-reactive immune cells from experimental metastatic tumor-sensitized mice. Also, phenotypic changes in tumors due to metastasis or tumor microenvironment influences were characterized. Metastatic neu+ mouse mammary carcinoma (mMMC) and its distant relapsing neu-antigen-negative variant (mANV) were investigated in FVBN202 mice. Tumor-reactive central memory CD8+ T cells and activated NK/NKT cells were successfully reprogrammed and expanded during 6-day expansion from mMMC- and/or mANV-sensitized mice, resulting in tumor-specific cytotoxicity. mMMC exhibited a flexible neu-expression pattern and acquired stem-like, tumorigenic phenotype

following metastasis while mANV remained stable except decreased tumorigenicity. Myeloid-derived suppressor cell (MDSC) levels were not increased. Adoptive cellular therapy (ACT) with reprogrammed tumor-reactive immune cells may prove effective prophylaxis against metastatic or recurrent breast cancer.

Introduction

The need for effective therapy against recurrent and metastatic breast cancer has been poorly addressed in recent years. The cancer-associated mortality from solid tumors due to metastatic disease has been estimated at 90% (1). As the overall numbers of patients with breast cancer decreases, the number of patients with advanced invasive breast cancers, refractory to conventional therapies, increases at a rate outpacing novel therapeutic development (1). In a study conducted from 1992 through 2007, a higher risk of death was associated with relapsed breast cancer patients following local treatment than in stage IV patients naïve to treatment, effectively separating these two groups for treatment considerations (2). Metastatic distant recurrent disease has been estimated in 2013 to occur in a quarter of breast cancer patients following adjuvant chemotherapy (3). As of this year, the estimated 24.3% 5-year rate of survival for women with distant metastatic disease at diagnosis is shockingly low when considering that 1 in 8 U.S. women will develop invasive breast cancer in their lifetime (4). Breast carcinomas with HER2/neu protein overexpression (Estrogen Receptor(ER)-, Progesterone Receptor(PR)-) have been estimated to comprise 25-30% of total tumors compared to luminal A (ER+ and/or PR+, HER2-), luminal B (ER+ and/or PR+, HER2+) and triple-negative forms (roughly 10-15%) of cancer based on receptor expression (1, 5). Mittendorf et al. found that 1/3 of HER2/neu+ breast cancer patients receiving neoadjuvant Trastuzumab lost HER2/neu expression and those patients had a much lower rate of recurrence-free survival (5). Both HER2/neu+ and triple-negative

basal-like forms of breast cancer have been associated with a poor prognosis and higher risk of disease recurrence (3, 5-7).

Metastasis has traditionally been thought of as a linear or parallel model of successful tumor relocation either sequentially or simultaneously with primary tumor growth within a patient (8). Metastases have demonstrated a tissue tropism in dissemination based on each primary neoplastic site that has become a signature for various forms of cancer according to a specific set of genes (9, 10). Breast cancer has demonstrated a preferential dissemination pattern to bone, lungs, brain and liver (10, 11). During dissemination, the tumors have been shown to undergo changes reminiscent of the embryogenic program of epithelial-to-mesenchymal transition (EMT) associated with progenitor cell trafficking during development and wound healing, along with the program reversal prior to secondary tumor establishment (MET). These EMT changes (12, 13) have major implications on adhesion, migration and ultimate survival that have been linked to a transition in breast carcinoma cells towards a stem-like phenotype (CD44+CD24-/low), originally discovered by Al Hajj et al. (14, 15).

The idea of tumorigenic cancer stem cells in breast cancer has been associated with self-renewal, enhanced tumor-initiation and treatment resistance (16-18). CD44 is an adhesion molecule found on the outside of most mammalian cells in various isoforms (often interacting with hyaluronic acid), involved specifically in rolling adhesion on activated lymphocytes and cell migration in other cells, including invasive metastatic tumor cells (19, 20). During metastatic disease progression, CD44 has been associated with the HER2 tyrosine kinase-signaling complex, indicating its importance in HER2/neu+ cells (20). CD24 is also an adhesion molecule found on many cell types that has been linked in breast cancer to p-selectin rolling adhesion and metastasis (21). The downregulation of CD24 during EMT has recently been linked to stress-

induced autophagy in CD44+CD24-/low mesenchymal-like breast cancer stem-like cells, reversed with autophagy inhibition towards the original epithelial-like phenotype (22). Santisteban et al. showed that CD8-dependent EMT also could induce stemness in breast cancer cells (23). Xie et al. determined that pro-inflammatory IL-6 could induce EMT in breast cancer cells (24). When considering the connections of EMT being associated with stem cell migration during wound healing, breast cancer cell stemness phenotype induction and multiple pro-inflammatory cytokines involved in the overall metastatic process, it is not surprising to consider the idea that progressive neoplasia has been associated with Th2-skewed chronic inflammation persisting in the tumor microenvironment (TME) instead of a productive Th1 anti-tumor response (25, 26).

The TME and its many cellular constituents, including macrophages and fibroblasts, have been implicated as initiators of cancer cell dissemination through the production of matrix metalloproteases (MMP) or expression of soluble angiogenic factors, if tumor cells are not inherently metastatic themselves (11). The results of mammary tumor dissemination studies have also inherently linked the ideas of TME crosstalk, metastasis and tumor dormancy, where disseminated cells may either successfully metastasize or become dormant (27). The proliferation and tumorigenicity of dormant tumor cells *in vitro* may be recovered upon retrieval from an incompatible site of metastasis, devoid of macroscopic metastatic formation (27). Tumor dormancy has raised many questions not well addressed by recent therapeutic advances. Previously, patients have been reported to develop recurrent disease 25 years after primary tumor resection (28). These cells may have been altered during EMT or the pre-metastatic niche may be incompatible with their growth requirements inducing a quiescent state that may be reversed at a later time by some triggering event (29).

Emerging uses for tumor immunotherapies have altered the way immunologists have approached the study of biologics in personalized healthcare. Trastuzumab and all related HER2/neu-specific passive immunotherapeutics introduced since 1998 have shown a positive effect of up to a 30% increase on ten-year overall survival and recurrence reduction up to 50% over previous chemotherapy regimens, especially in combination (5, 30). However when considering the distant recurrence-free interval following various treatments, little progress has been made in the past 30 years (3). Major advances to studies on metastasis have recently been made, including: mouse model developments (31), tracking tumors during the metastatic cascade (27, 32), monitoring disease progression and assessing the specific treatment effects of various therapies during the many steps of metastasis at different locations (11). But larger strides still need to be made in accurately quantifying phenotypic, genetic or epigenetic changes to the tumors as a result of metastasis in relation to immune responses.

Adoptive cellular therapy (ACT) has been employed to treat tumors by immune cell infusion requiring a strong T cell response for resolution following *ex vivo* expansion of T cell subsets of interest and often lymphodepletion (33). Adoptive immunotherapy has had limited patient success in solid primary tumors apart from complete regression of highly-immunogenic melanoma (34), but the use of ACT of *ex vivo* reprogrammed tumor-reactive immune cells in metastatic stage IV or recurrent breast cancer has only recently been considered (35-38). Some major therapeutic challenges with aggressive breast tumors have been: treatment resistance (acquired following Trastuzumab), circulating tumor cells resulting in distant metastases, tumor dormancy, and HER2/neu receptor loss towards the basal-like triple-negative invasive form (5, 11). Immunotherapy has had to overcome multiple treatment barriers also, including: low immunogenicity of tumors, immunosuppressive cells, low avidity/weak tumor-reactive immune

cell expansion and tumor stromal infiltration (33, 39). Immunosuppressive cells, like myeloid-derived suppressor cells (MDSCs) and/or T regulatory cells, have been implied in immunoediting tumors towards recurrence and promoting metastasis in multiple breast cancer models (36, 40-46). Increases in MDSC levels have been correlated with metastatic breast cancer in 4T1 spontaneous lung metastatic and MDA-MB-231 lymph node metastatic mouse models (40, 43, 44, 47) along with our primary mouse mammary carcinoma (MMC) model following tumor-derived soluble factor release, like GM-CSF (48). In order to combat immune evasive techniques and effectively clear these moving targets from the vasculature or lymphatics following conventional therapy, new personalized treatment plans are needed to address the complexities associated with metastatic breast carcinoma.

Our group has previously successfully reprogrammed tumor-reactive immune cells from FVBN202 mice (45, 46) towards a memory T cell and activated NK/NKT differentiated phenotype using Bryostatin 1 (49, 50) and Ionomycin (51, 52) with sequential common γ–chain cytokines (IL-2, IL-7 and IL-15) when challenged with MMC subcutaneously (s.c.) for use in prophylactic ACT of primary solid tumor. Ultimately, activated NK/NKT cells induced MDSC resistance and rescue of cytotoxic CD8+ T cell functions to produce tumor regression along with a memory response upon repeat challenge with primary tumors (46). Also, we have shown that IFN-γ treatments of MMC could induce relapse (HER2/neu loss) to an antigen-negative variant (ANV) by hypermethylation of the mouse mammary tumor virus (MMTV) promoter, directly epigenetically regulating HER2/neu and IFN-γRα expression (53). In our current study, we wanted to apply some of the techniques already described in a more clinically relevant model of therapy, metastatic or recurrent breast cancer. We compared neu-protein overexpressing MMC with relapsed ANV, similar to basal-like triple-negative invasive human breast cancer, prior to

and directly following metastatic cascade as a means to understand some of the therapeutic problems previously listed in a relevant immune setting, HER2/neu-overexpressing FVBN202 transgenic mice. The objectives of the study were to: i) test the feasibility of *ex* vivo expansion and reprogramming of tumor-reactive immune cells from mMMC- or mANV-sensitized FVBN202 mice for determination of functional efficacy at cytotoxic tumor-killing *in vitro*, and ii) determine the role of metastatic cascade or microenvironment influences at inducing tumor phenotypic changes. Previously, our group (54) investigated the neu-specific anti-tumor immune response in the context of vaccine or ACT design. Disis and colleagues have also produced an effective peptide-based vaccine targeted at HER2/neu oncoprotein extracellular domains resulting in prolonged overall survival in concert with Trastuzumab treatment (55, 56). These immunotherapeutic strategies employed may be combined with drugs that target the pre-metastatic niches to effect changes that may prove incompatible with the growth patterns of circulating tumor cells upon arrival at a secondary site (11). Our study elucidated the feasibility of *ex* vivo expansion and reprogramming of tumor-reactive immune cells with cytotoxic efficacy despite metastatic or TME influences. This assisted in the proposal of a new preventive treatment option for the future of synergistic, long-term metastatic breast cancer therapy, which may be initiated following conventional treatment of primary tumor instead of or possibly in addition to the established metastatic disease treatments currently employed.

Methods and Materials

Mouse model

FVBN-202 female transgenic mice (Charles River Laboratories) between the ages of 6 and 16 weeks were used throughout these experiments. FVBN-202 mice overexpress the unactivated rat neu transgene in mammary glands under the control of MMTV promoter with the potential for pulmonary metastatic disease after long latency (57). The normal disease progression in older mice starts with pre-malignant hyperplasia most like ductal carcinoma in situ (DCIS) and increased endogenous myeloid-derived suppressor cell (MDSC) levels before spontaneous mammary carcinoma develops (54). All studies were reviewed and approved by the Institutional Animal Care and Use Committee (IACUC) at Virginia Commonwealth University.

Tumor cell lines

The neu overexpressing mouse mammary carcinoma (MMC) cell line was established from a spontaneous mammary tumor harvested from FVBN202 mice (58). The antigen negative variant (ANV) form was derived from MMC tumor cells under neu-specific immune pressure in Parental FVB mice (59). To establish experimental lung metastasis, mice were challenged with 1 x 10^6 primary tumor cells by tail vein injection (i.v.) for 22-29 days based on changes in

moribundity or drops in weight. Lung metastases were surgically excised upon animal sacrifice under aseptic conditions. The lungs were photographed and finely minced prior to cold tryspinization with 0.25% Trypsin in HBSS for 12-16 hours at 4°C. Following overnight incubation, the cell suspension was gently vortexed and incubated for 30 minutes at 37°C, 5% CO_2 prior to straining cells through 70 micron strainers (BD, San Jose, CA) for culture (60). Single cell suspensions were achieved with substantial mechanical disaggregation of clumps by pipetting cells with decreasing sized pipet tips for many minutes. Differential trypsinization over multiple passages allowed for tumor cell purification using 0.05% Trypsin in PBS for 3 minutes by fibroblast removal. Metastatic MMC (mMMC) and metastatic ANV (mANV) were established over a month supplemented with 20% FBS for purification/ fibroblast removal prior to full characterization. To test phenotypic changes acquired during metastasis, 3-5 x 10^6 metastatic or control primary cells were inoculated by subcutaneous (s.c.) challenge into the groin region. Primary tumors from mice burdened with bulky mammary subcutaneous tumors were surgically excised upon animal sacrifice under aseptic conditions. Primary tumors (from previously established cell lines) were processed similar to metastatic lungs, except that the reisolated cells were only allowed to adhere to flasks for 3-5 days prior to flow cytometric analysis. Tumor cells were normally maintained in RPMI 1640 media supplemented with 10% FBS. Fold growth was determined by change in cell number from original optimal seeding amount (final cell number/ seeded cell number). Tumor cell passaging utilized 2.5 mM EDTA in PBS (mMMC & MMC) to minimize active suspension tumor aggregate formation or 0.25% Trypsin in HBSS (mANV & ANV) normally. All cell counts were performed with trypan blue exclusion for viability determination. Freezer stocks were created for future study of newly established metastatic cells (2 x 10^6 cells, 90% FBS + 10% DMSO).

Flow cytometry

Flow cytometric analyses were performed as previously described by our group (46). Briefly, spleens or tumors were disaggregated into a single cell suspension (above) and 10^6 cells were aliquoted into each sample tube. Red blood cells were lysed for removal from spleens with ACK Buffer (Quality Biological, Gaithersburg, MD) and washed twice to purify viable cells. Non-specific binding of antibodies (Abs) to Fc Receptors (FcR) was blocked by incubating the cells with anti-CD16/32 Ab on ice for 20 minutes per the manufacturer's recommendation (BioLegend, San Diego, CA). Cells were stained with surface Abs toward various markers and incubated on ice in the dark for 20 min. The cells were then washed with cell staining buffer (PBS, 1% FBS, 0.1% sodium azide) and fixed with 1% formaldehyde. For Annexin V staining, cells were stained for respective surface markers, washed with cell staining buffer, and then washed with 1X Annexin V buffer (BD Pharmingen, San Jose, CA). The Annexin V and propidium iodide (PI) staining protocol given in the product data sheet was then followed. Abs used for flow cytometry were purchased from BioLegend (FITC- Goat anti-mouse IgG1, FITC-, PE/Cy5-CD3, PE/Cy5-, allophycocyanin-CD4**,** FITC-, PE-, PE/Cy5-CD8, FITC-, PE-CD11b, FITC-, PE-Gr1, FITC-, PE-CD25, PE-CD44, allophycocyanin-CD62L, allophycocyanin-CD49b, PE/Cy5-CD69, PE-CD122, and PE-CD127, PE/Cy5-CD24). All Abs were used at the manufacturer's recommended concentrations. Multicolor data acquisition was performed immediately for viability studies or within 24 hours of fixation on a BD FACSCanto II. Analysis was performed using BD FACSDiva software or FlowJo Software (Treestar, Ashland, OR).

MTT proliferation assay

MTT proliferation assay was performed according to the manufacturer's protocol (Roche, Mannheim, Germany). An optimization plate revealed the most even proliferation from all cells was at a cell density of 5 x 10^3 cells per well. Tumor cells were plated on 96-well plates at 5 x 10^3 cells per well for 48-hour culture at 37°C, 5% CO_2 prior to addition of MTT reagent. MTT reagent was added for a 4-hour incubation for formazan crystal formation prior to overnight incubation with HCl solubilization solution. Samples were read on an ELISA plate reader at a wavelength of 540 nm and negative control wells that did not receive MTT were subtracted as reference to remove assay background absorbance. Five wells were plated for each cell type for statistical analysis.

Invasion assay

Boyden chamber Matrigel (BD Biosciences, Bedford, MA) invasion assays were performed essentially as previously described (61). Cells in 200 uL growth media were added to cell culture inserts (0.8 μm pore) coated with Matrigel (diluted 1:6 in cell growth medium, dried for 30 min. at 37°C, 5% CO_2) on a 24 well plate (BD Falcon, Franklin, NJ) and 300 uL growth media was added to the lower chamber. Analysis of invading tumor cells consisted of seeding the cells at 2 x 10^4 – 1 x 10^5 cells per well for 48 hour culture at 37°C, 5% CO_2. Tumors were tested for presence or absence of Matrigel invasiveness following fixation with 5% Glutaraldehyde (Ted Pella, Redding, CA) and toluidine blue staining (0.5%). Assessment of the ability to invade at different concentrations was determined by picture representations of each cell type.

Ex vivo expansion of tumor-sensitized immune cells from FVBN202 mice

FVBN202 transgenic mice were injected intravenously (i.v.) with tumor cells, and splenocytes were harvested after 16–29 days based on tumor burden or weight loss/ moribundity in experimental metastatic mice. Tumor growth from subcutaneous inoculation was monitored by digital calipers, and tumor volumes were calculated by volume (v) = (L [length] × W [width]^2)/2. Splenocytes (10^6 cells/ml) were stimulated upon harvest in complete medium (RPMI 1640 supplemented with 100 U/ml penicillin, 100 mg/ml streptomycin, 10% FBS, 10 mM L-glutamine) containing 10% FBS as well as bryostatin 1 (5 nM)/ionomycin (1 μM), and 80 U/ml IL-2 for 16 h (B/I + IL-2), as previously described by our group (46). Cells were then washed three times and cultured at 10^6 cells/ml in complete medium with 20 ng/ml each of common γ-chain cytokines (γ-c), IL-7 and IL-15 (PeproTech, Rocky Hill, NJ). After 24 h, 20 U/ml IL-2 was added to the culture. On the next day, cells were washed three times and cultured at 10^6 cells/ml in complete medium with 40 U/ml IL-2. Cells were counted and cultured as before with 40 U/ml IL-2 every other day for a total of 6-7 d. After day 6-7, cells were used for *in vitro* studies.

IFN-γ ELISA

ELISA was performed as previously described by our group (46). Briefly, *ex vivo* expanded tumor-primed splenocytes were cultured in complete medium at a ratio of 10:1 with irradiated MMC, mMMC, ANV or mANV cells (14,000 rad) for 24 h. Supernatants were collected and stored at -80°C until assayed. IFN-γ was detected using a Mouse IFN-γ ELISA kit (BD Pharmingen, San Jose, CA) according to the manufacturer's protocol.

Cytotoxicity assay

In vitro cytotoxicity assay was performed as previously described by our group (46). Briefly, *ex vivo* expanded tumor-primed splenocytes were cultured with MMC, mMMC, ANV or mANV cells at a 10:1 E:T ratio in 5 ml growth medium with 20 U/ml IL-2 (PeproTech, Rocky Hill, NJ) in 60 x15 mm individual culture dishes (Greiner). After 48 h, cells were harvested and stained for neu (anti–c-Erb2/c-Neu; Calbiochem, San Diego, CA), CD3, Annexin V, and PI according to the manufacturer's protocol (Biolegend, San Diego, CA). Flow cytometry was used to analyze the viability of neu+ MMC or mMMC, CD3- Tumors (all four) or CD3+ T cells for clear separation of tumor-specific killing or activation induced cell death (AICD).

Statistical analysis

Graphical data are presented as means with standard errors (SEM) where possible. Statistical comparisons between groups were made using paired (treated) or unpaired (untreated) one-tailed, unequal variance student's t tests with $p < 0.05$ considered statistically significant.

Results

Lung metastatic mMMC and mANV exhibited enhanced proliferation and a similar morphology compared to primary MMC and ANV tumor cells

Upon experimental lung metastasis of neu positive mouse mammary carcinoma (MMC) and its relapsing neu antigen negative variant (ANV), mMMC and mANV tumor cell lines were established for characterization of phenotypic changes following the metastatic cascade. As seen in Figure 1A, lung metastatic disease induced by intravenous injection of MMC or ANV showed significant macro-metastatic pulmonary disease. Growth of mMMC resulted in diffuse bulky tumor formation in the lungs within 23.6 days on average (n=5). The nodular growth of mANV resulted in pronounced lung deterioration and clotting upon sacrifice within 28.5 days on average (n=2). The time for macrometastasis formation in the lung requiring sacrifice (Figure 1B) was significantly shorter in FVBN202 mice bearing MMC compared to mice bearing ANV ($p=0.002$). Significant increases in proliferation of the metastatic cells were shown in Figure 1C by MTT assay ($p<0.001$) compared to primary tumor cells for each tumor type, along with the characteristic difference of ANV proliferation increased over MMC. The growth of mMMC shown in Figure 1D exhibited a small, rounded shape growing in mounds upward instead of the more cubical primary MMC growing as a monolayer, radiating outward. The growth of mANV retained a spindled basal-like mesenchymal phenotype. The overall morphology of mMMC and mANV following metastasis were similar to primary MMC and ANV tumor, respectively.

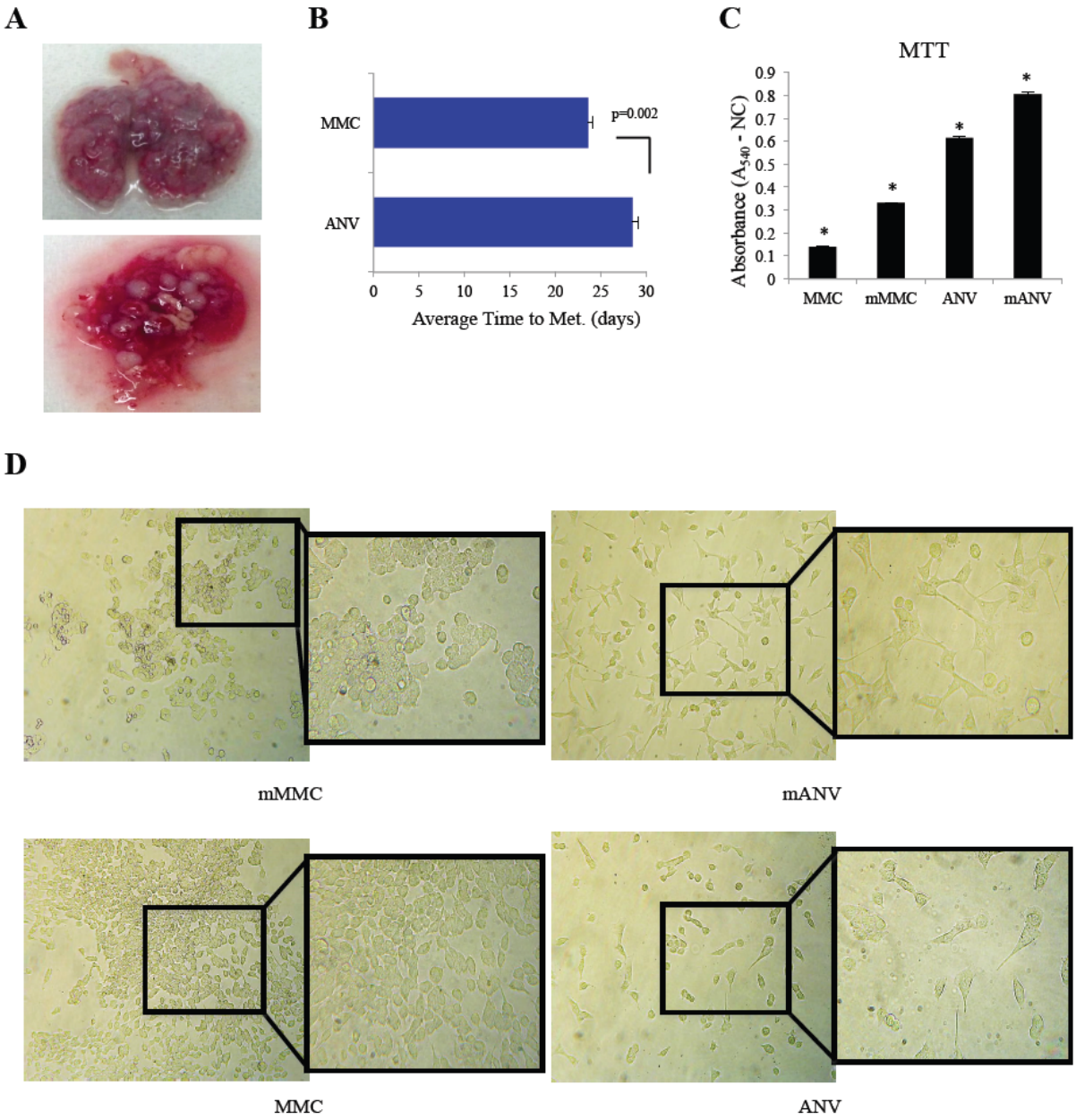

Figure 1. Experimental metastatic disease of primary MMC and relapsing ANV results in enhanced proliferation and a similar morphology. (A) Pulmonary metastatic disease following tail-vein tumor challenge of MMC (Top) or ANV (Bottom). (B) Average time to metastasis formation requiring sacrifice following intravenous challenge with MMC (n=5) or ANV (n=2) was determined. Error bars represent standard error of the mean. Significance considered for student's t-test result of $p<0.05$ (Bar indicates a significant difference). (C) MTT proliferation data from mMMC, MMC, mANV, and ANV was shown following culture for 48 hours with five well repeats averaged per tumor. Absorbance was recorded at 540 nm and negative control wells subtracted as background. All tumors were significantly different from each other assessed by one-tailed, unequal variance student's T-test (*$p<0.001$). (D) Morphological features of tumor cells *in vitro* were photographed (left panel: 10X magnification; right panel: 25X selection zoom): mMMC, mANV, MMC and ANV.

CD44+CD24-/low stem-like phenotype was established simultaneously with enhanced neu-expression in mMMC during lung metastasis

Since relapsed ANV had characteristics of stem-like cells (7), we sought to determine whether establishment of primary tumor cells in the lung might result in the acquisition of a stem-like phenotype in MMC. As shown in Figure 2, mMMC acquired a stem-like phenotype in the lung by showing loss of CD24 expression (from 89.4% in MMC to 9.09% in mMMC) despite a universal upregulation of neu-protein (from 8.53% in CD24- MMC to 98.1% in CD24- mMMC; from 77.7% in CD24+ MMC to 99.3% in CD24+ mMMC). Retention of neu expression during CD24 loss suggests that loss of CD24 in mMMC was not merely due to the selection of CD24- phenotype from within the heterogeneous MMC population. Primary ANV (CD44+CD24-, 73.8%) and mANV (CD44+CD24-, 79.5%) exhibited a similar phenotype upon comparison indicating a stable lack of neu expression and stem-like metastatic phenotype.

The invasive capacity of ANV remains stable following metastasis

In order to address the metastatic potential of mammary tumor cells, invasiveness was considered for MMC and ANV prior to and directly following metastasis. Boyden chamber invasion assay through Matrigel indicated positive invasion for mANV and ANV (Figure 3B & 3C) while mMMC and MMC exhibited no invasion (Figure 3A & 3C). For comparison of cells before and after metastasis, ANV invasiveness remained stable following metastatic cascade while MMC exhibited poor or very low invasiveness without effect from metastasis. Positive invasion (Figure 3D) was evaluated by toluidine blue staining of cells that had successfully

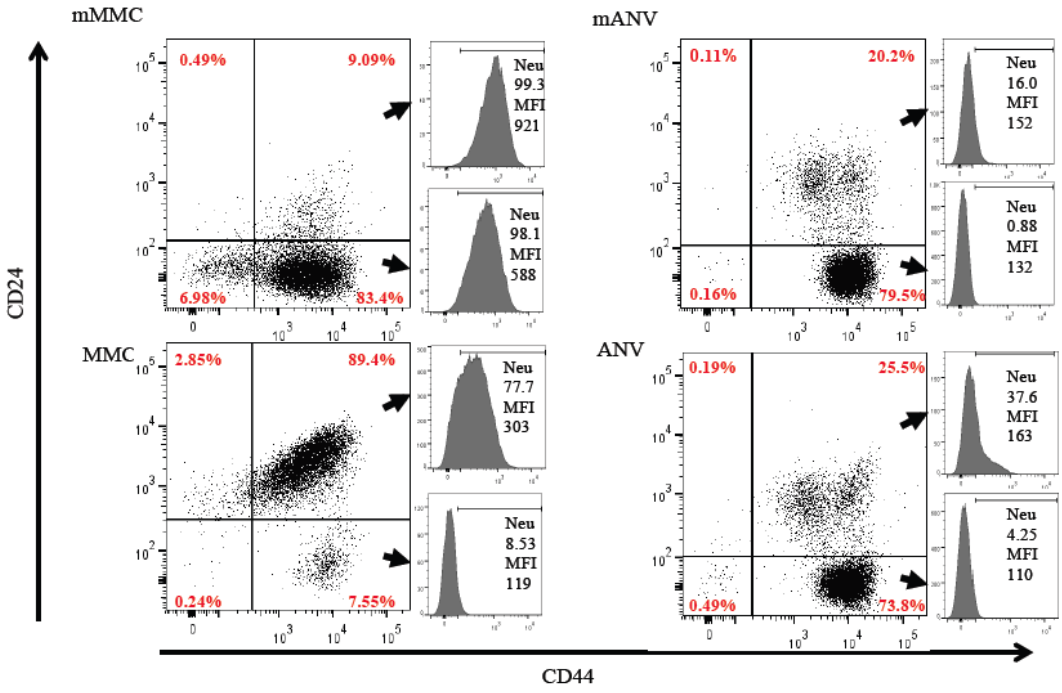

Figure 2. Stem-like characteristics were acquired by tissue-specific means during experimental metastasis of primary MMC. Experimental metastatic and primary tumor cell analysis were completed for CD24 and CD44 expression. Arrows indicate neu protein expression in gated CD24+ or CD24- populations. Representative data shown (n=1 biological repeat for each metastatic cell line established for study; repeat screenings of cultured metastatic cells confirm findings).

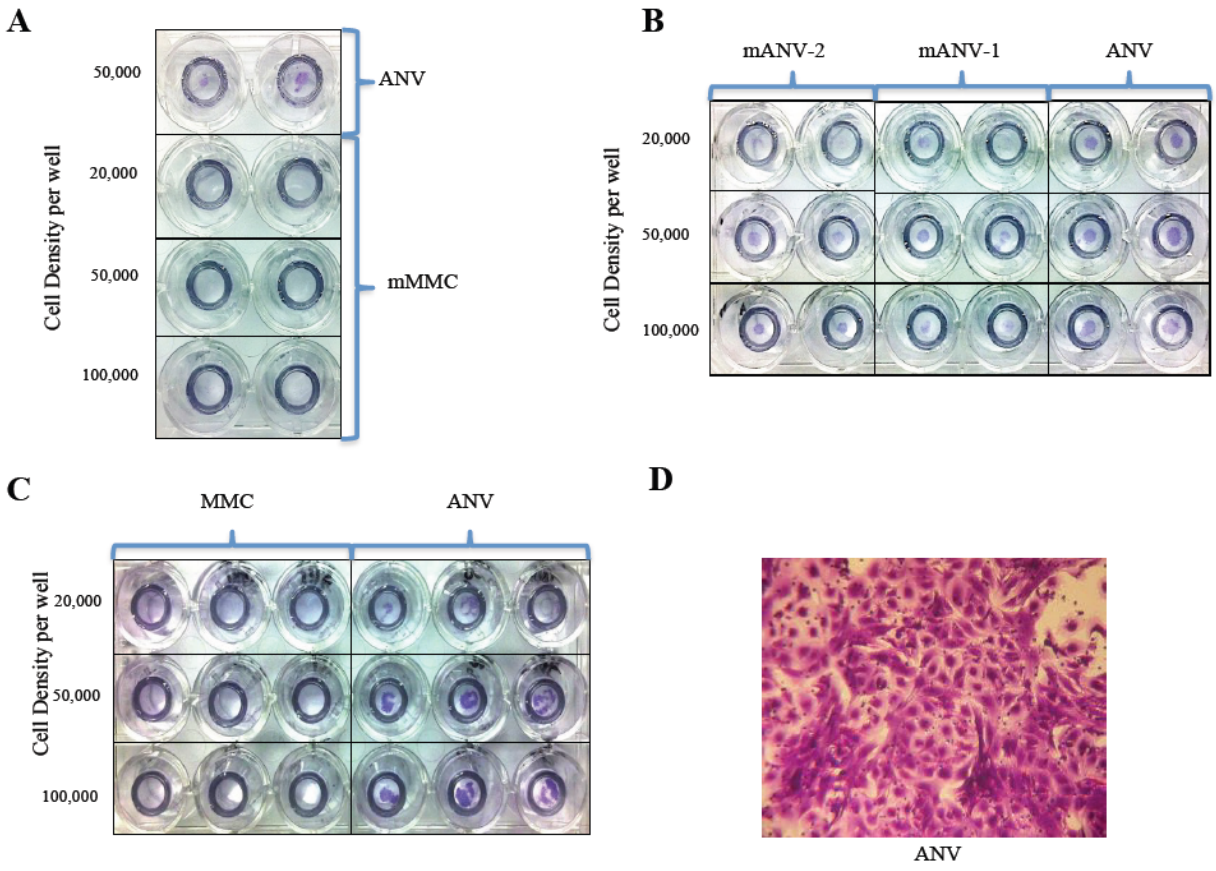

Figure 3. The invasive capacity of ANV remains stable following metastasis. (A) Boyden chamber invasion assay through Matrigel was performed to determine the invasiveness of mMMC cells (Positive Control (PC) =ANV). (B) Invasion assay of mANV cells from two mice confirmed invasiveness (PC=ANV). (C) Invasion assay for primary MMC and relapsing ANV tumor cells assessed invasiveness prior to metastasis for baseline comparison. (D) 25X magnification of invaded cells from ANV primary were fixed with glutaraldehyde and stained with toluidine blue.

broken down the Matrigel layer and migrated through 0.8 μm pores to the opposite side of the Boyden chamber during 48-hour growth. As this assay only tests for the breakdown of Type I/IV collagen present in basal membranes followed by successful migration, it is not considered representative of all forms of invasion, but merely just single-cell invasive means instead of collective or extracellular-mediated (macrophage or fibroblast) methods (62).

MDSC levels were minimal in FVBN202 mice bearing lung metastatic mMMC or mANV tumor

Since tumor-derived soluble factors raise MDSC levels *in vivo* (48), we investigated whether mMMC or mANV may also increase splenic MDSC trafficking. MDSC levels were not increased in experimental metastatic mice (Figures 4A). The MDSC levels in mANV (9.3%) or mMMC (21.2%; n=3) experimental metastatic mice (Figure 4B) were lower than previously reported in mice challenged with MMC primary tumor (45). Splenomegaly was not observed in experimental metastatic mice, further supporting a drop in MDSC levels (Figure 4C).

Tumor-reactive splenocytes can be expanded and reprogrammed from FVBN202 mice bearing lung metastatic mMMC or mANV

In order to address the use of B/I + γ-c cytokines in the expansion of metastatic tumor-sensitized lymphocytes, splenocyte expansion efficiency and tumor-specific IFN-γ production were assessed for the experimental metastasis model (Figure 5). One day after B/I + IL-2 treatment, a sharp drop was observed in the number of splenocytes from mMMC- sensitized ($p=0.022$) and mANV-sensitized mice ($p=0.013$), as previously seen by our group during

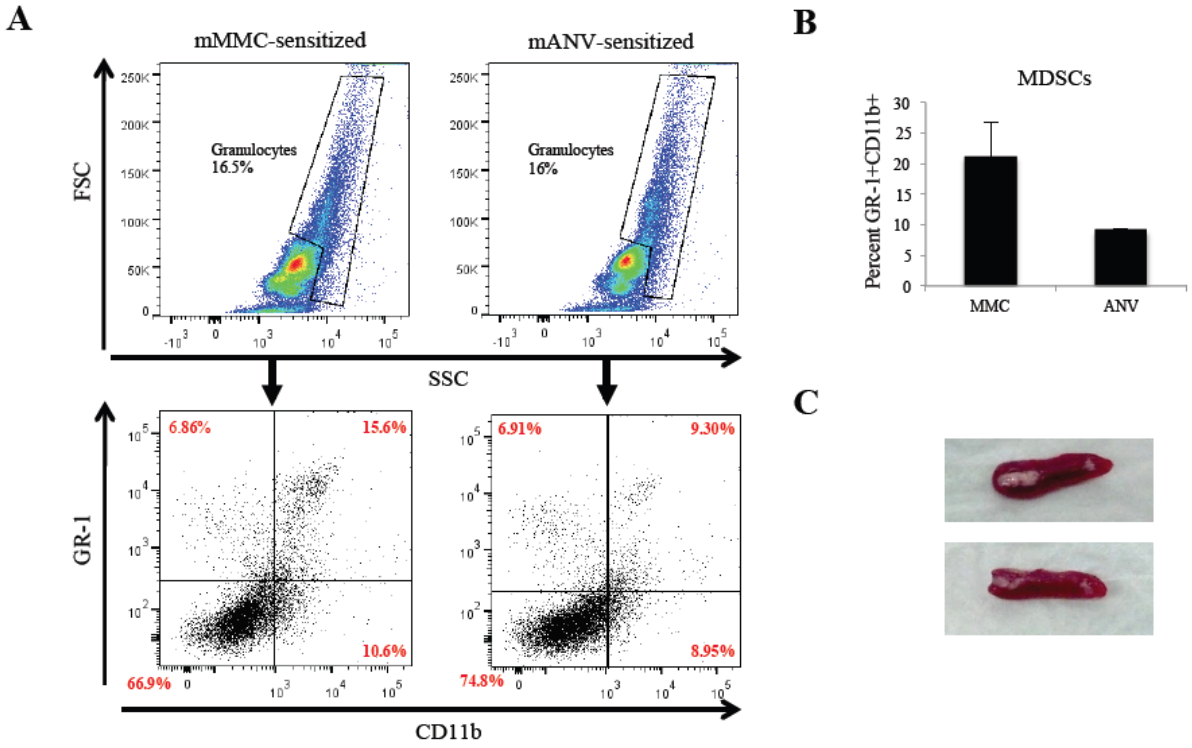

Figure 4. Splenic MDSC accumulation in experimental metastatic mice was minimal. (A) Experimental metastatic mouse splenocytes were stained for GR-1+CD11b+ MDSCs as percent of total granulocytes. Representative plots shown. (B) The percentage of splenic MDSCs was determined on gated granulocyte population of mice bearing mMMC (n=3) or mANV (n=1). Error bars represent standard error of the mean. (C) Spleen size was considered normal in metastatic mice (mMMC, Top; mANV, Bottom).

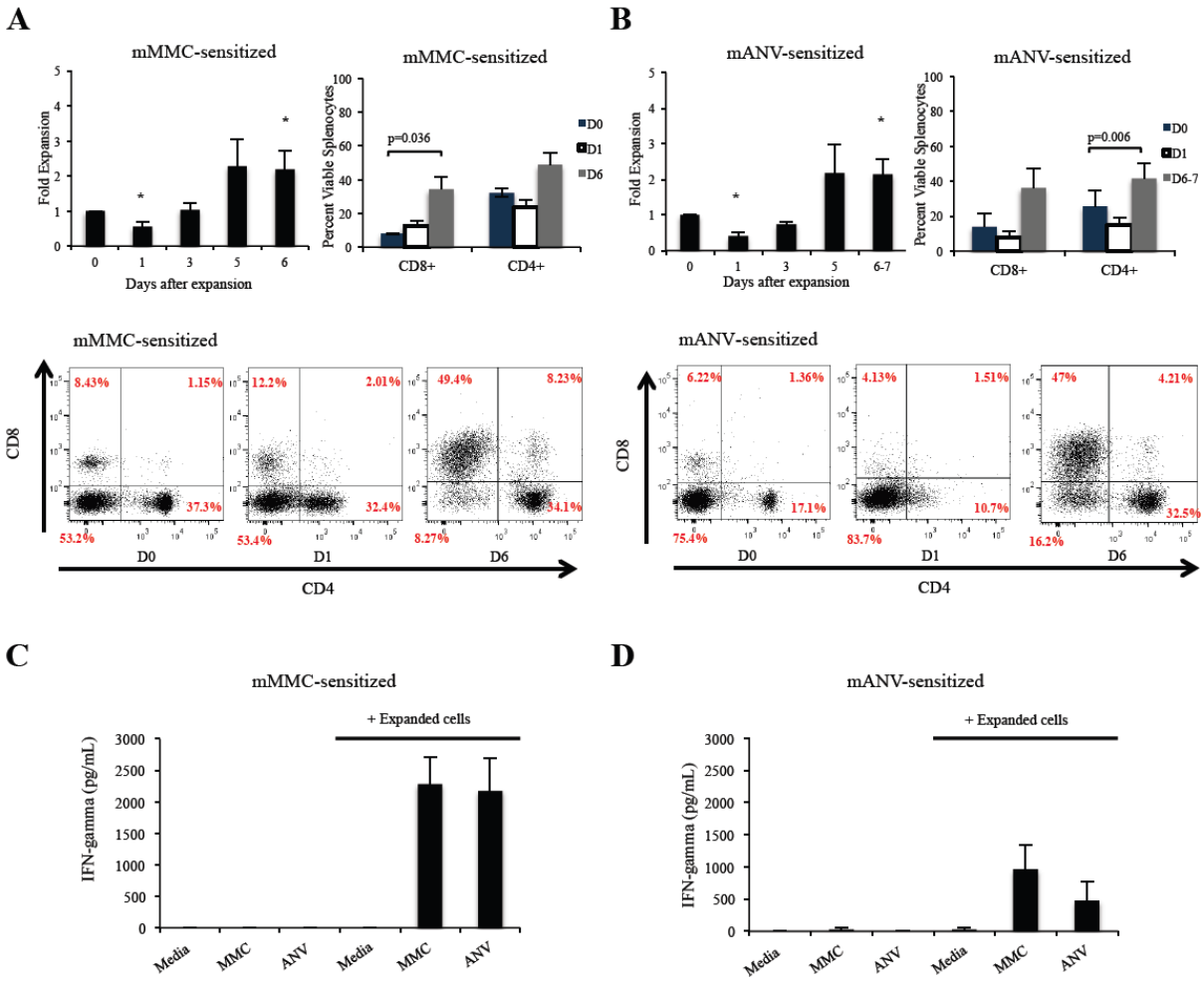

Figure 5. ***Ex vivo*** **expanded, tumor-sensitized splenocytes produce IFN-γ following experimental metastasis.** (A) Fold expansion of splenocytes from mMMC-sensitized mice with B/I and γ-chain cytokines (upper left panel) was quantified by trypan blue exclusion (n=4) or flow cytometric analysis of CD8+ and CD4+ splenocytes (n=3) with average (upper right panel) and representative data shown (bottom panel). Significance (*) considered for student's t-test result of $p<0.05$ (Bars/p-values indicate trends of notable significance: bracket, D0 vs D6-7). (B) Fold expansion of splenocytes from mANV-sensitized mice (upper left panel) was also assessed (n=3) or flow cytometric analysis of CD8+ and CD4+ splenocytes (n=2) with average (upper right panel) and representative data shown (bottom panel). (C) Tumor-specific IFN-γ production was determined by ELISA of supernatants from splenocytes of mMMC-sensitized mice (n=2). Duplicate wells were averaged. (D) Tumor-specific IFN-γ production was also determined by ELISA of supernatants from splenocytes of mANV-sensitized mice (n=3; for cross-reactivity against MMC, n=2).

activation and reprogramming to indicate only tumor-antigen-primed cells were expanded (46). Splenocytes were successfully expanded on average from mMMC-sensitized mice (2.2-fold expansion by day 6) and mANV-sensitized mice (2.1-fold expansion by day 6) using B/I + γ-c cytokines over 6-7 days (Figure 5A & B, left upper panels). A 6-7 day culture of splenocytes with common γ-chain cytokines resulted in the notable expansion of splenocytes from mMMC-sensitized ($p=0.017$) and mANV-sensitized mice ($p=0.008$). A moderate expansion of CD8+ and CD4+ T cells was observed in Figure 5A & B (upper right and lower panels) by exhibiting a 1.5- to 4-fold expansion, similar to previous results of *ex vivo* expansion of primary tumor-reactive splenocytes (46). Average CD8+ T cells increased overall during 6-7 day expansion from mMMC-sensitized (8.12% (D0) vs. 34.4% (D6); $p=0.036$) or mANV-sensitized mice (14.01% (D0) vs. 36.1% (D6-7)). Despite fluctuation following B/I + IL-2 from day 0 to day 1, average CD4+ T cells also increased overall during 6-7 day expansion from either mMMC-sensitized (32.2% (D0) vs. 48.8% (D6-7)) or mANV-sensitized mice (25.7% (D0) vs. 41.4% (D6-7); $p=0.006$). The specific variation shown by error bars (SEM) between mANV-sensitized mice ($n=2$) for average CD8+ or CD4+ T cells was observed simultaneously with an uncommon viability fluctuation in one mouse, from 95% viability at day 0 to 34% viability at day 1 rebounding to 92% by day 7. Splenocytes expanded from mMMC-sensitized mice also showed IFN-γ production in Figure 5C against MMC and ANV tumors (average, 2279 pg/mL and 2176 pg/mL, respectively). By comparison, expanded splenocytes from mANV-sensitized mice showed less IFN-γ production in Figure 5D against ANV and MMC tumors (average, 494 pg/mL and 964 pg/mL, respectively). IFN-γ production of splenocytes was positively indicated in response to tumor co-culture from both, mMMC- and mANV-sensitized mice but sample variation at this early time in the pilot study ($n=2$, mMMC-sensitized; $n=3$, mANV-sensitized

mice - for cross-reactivity against MMC, n=2) precluded any claims of significance being drawn.

Phenotype analysis of expanded splenocytes over 6-7 days revealed the efficiency of reprogramming anti-tumor immune cells from experimental metastatic mice (Figures 6-8). Figure 6 depicts a notable reduction of CD62L+ T cells (including CD44-CD62L+ naïve T cells (T_N), CD44+CD62L+(low) effector memory T cells (T_{EM}) and CD44+CD62L+(high) central memory T cells (T_{CM})) along with the enhancement of CD44+CD62L- effector T cells (T_E) following B/I + IL-2 treatment on day 0 to day 1, supporting successful T cell reprogramming. A general downregulation of CD62L expression from 81.9% on day 0 to 69.7% on day 1 was seen in Figure 6A (lower left panel) in average mMMC-sensitized mice (p=0.00006). CD62L downregulation was absent from average mANV-sensitized CD8+ T cells in Figure 6B, but they exhibited a similar specific trend of reduction of average CD8+ T_N cells (lower right panel) from 19.9% on day 0 to 1.42% on day 1. CD62L downregulation was also observed in Figure 6C in average mMMC-sensitized CD4+ T cells from 75.9% at day 0 to 20.9% at day 1 (p=0.006). CD4+ T cells from mANV-sensitized mice exhibited a similar trend of CD62L downregulation from 79.8% on day 0 to 35.4% day 1 (n.s.) in Figure 6D despite a high level of sampling variation, supported by a notable reduction of CD4+ T_N cells (16.1% to 4.96%; p=0.033). Also, average CD8+ T_E cells increased from day 0 to day 1 in Figure 6A from mMMC-sensitized mice (9.98% to 15.9%; p=0.031) and in Figure 6B from mANV-sensitized mice (40% to 50.9%; n.s.). An increase in average CD4+ T_E cells was similarly observed from day 0 to day 1 in Figure 6C in mMMC-sensitized mice (20.3% to 69.3%; p=0.009) and in Figure 6D from mANV-sensitized mice (18.2% to 60.9%; n.s.). Further, a strong reprogramming and phenotypic differentiation by day 6 towards a central memory T cell (T_{CM}) phenotype in mMMC-sensitized and mANV-sensitized mice was exhibited in Figure 6, concurrent with a noticeable drop in effector memory

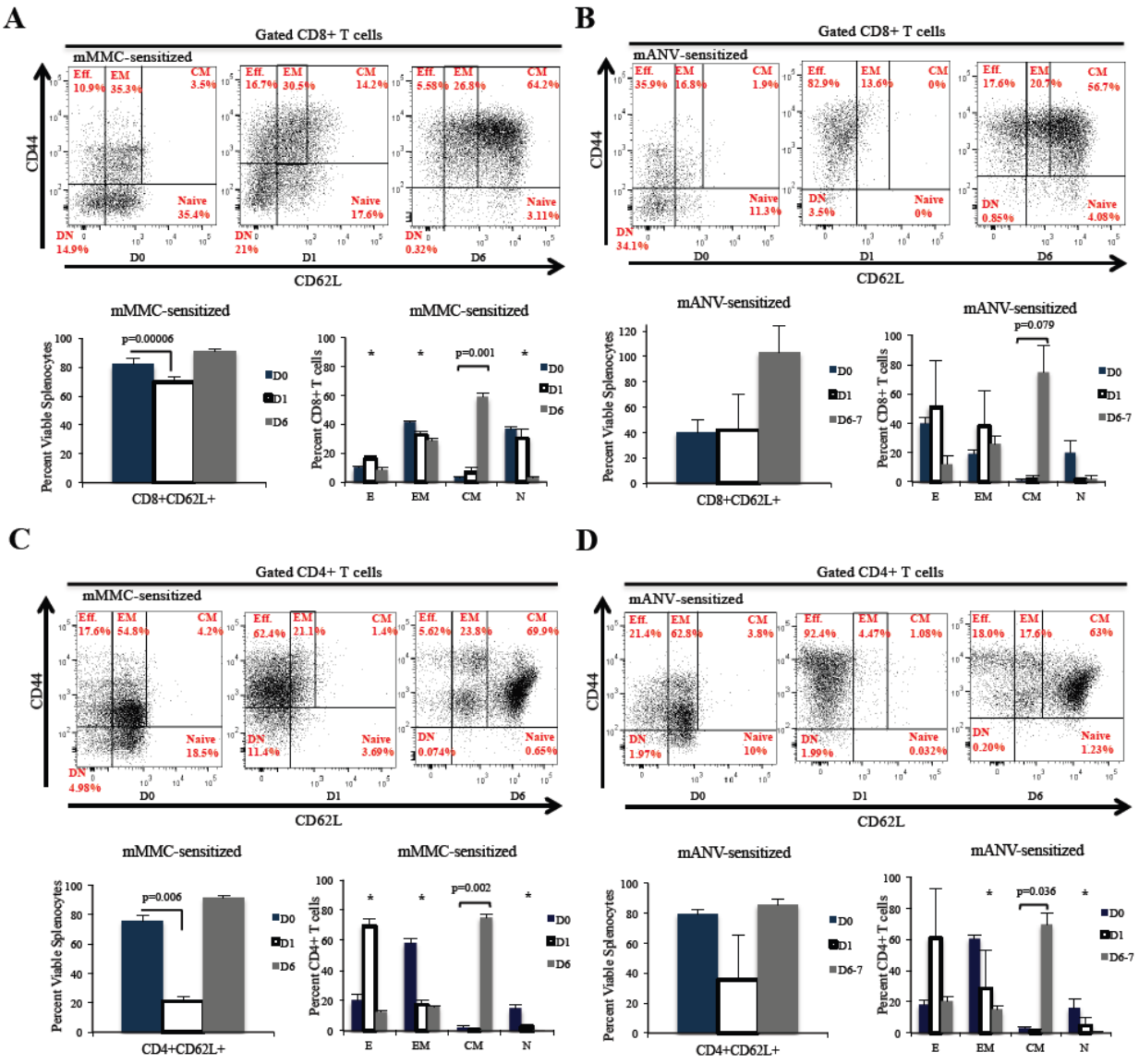

Figure 6. Metastatic mice exhibit responsive expansion and reprogramming of memory CD8+ or CD4+ T cells during 6-7 day culture. (A) CD44+CD62L- effector (E), CD44+CD62L+/low effector memory (EM), CD44+CD62L+/high central memory (CM), CD44-CD62L+ naïve (N) and double negative (DN, CD44-CD62L-) CD8+ T cell phenotypes or general CD8+CD62L+ T cells were determined from flow cytometric analysis of mMMC-sensitized splenocytes over the course of expansion (n=3). Representative (upper panel) and averaged data (lower panels) shown. Significance (*) considered for student's t-test result of $p<0.05$ (Bars/p-values indicate trends of notable significance: pointing left, day 0 (D0) vs. D1; bracket, D0 vs. D6-7). (B) CD8+ T cell phenotypes (E, EM, CM, N, DN) or general CD8+CD62L+ T cells were also determined from mANV-sensitized splenocytes (n=2). (C) CD4+ T cell phenotypes (E, EM, CM, N, DN) or general CD4+CD62L+ T cells were similarly assessed from mMMC-sensitized splenocytes (n=3). (D) CD4+ T cell phenotypes (E, EM, CM, N, DN) or general CD4+CD62L+ T cells were also quantified from mANV-sensitized splenocytes (n=2).

T cells (T_{EM}) and naïve T cells (T_N), as previously seen (46). Average CD8+ T_{CM} cells were expanded by day 6 from baseline from both, mMMC-sensitized (Figure 6A, 59%; p=0.001) and mANV-sensitized mice (Figure 6B, 74.8%; n.s.). Average CD4+ T_{CM} cells were also expanded by day 6 from baseline from both, mMMC-sensitized (Figure 6C, 75%; p=0.001) and mANV-sensitized mice (Figure 6D, 69.8%; p=0.036).

In order to evaluate the splenocyte activation status in response to 6-7 day expansion, CD25 and CD69 expression levels were investigated. The activation events induced by B/I+IL-2 were seen on day 1 for CD8+ and CD4+ T cells by CD25 expression (2- to 10-fold increases in average CD25+ cells) and sustained until day 6 as shown in Figure 7 (A-D). CD25+ activation events were clearly discerned from mMMC-sensitized mice in Figure 7A in average CD8+CD25+ T cells from 14.2% on day 0 increasing to 82.3% on day 1 (p=0.008) persisting to day 6 (66.3%; p=0.007, D0 vs. D6). Average CD4+CD25+ T cells from mMMC-sensitized mice in Figure 7B also increased from 7.39% on day 0 to 80.1% on day 1 (p=0.002) persisting to day 6 (85.6%; p=0.001). By comparison, activation trends were also discerned from mANV-sensitized mice in Figure 7C in average CD8+CD25+ T cells increasing from 24.6% on day 0 to 49.7% on day 1, stable to day 6-7 (48.7%). The aforementioned technical issue of fluctuating viability at day 1 in splenocytes from one mANV-sensitized mouse may be considered the cause of the difference observed between the high values of representative data shown in the left panel of Figure 7C for CD8+CD25+ T cells and the lower averaged data on the right with large error bars to indicate this notable variation, presumably also affecting comparative statistical analysis. Average CD4+CD25+ T cells from mANV-sensitized mice also comparably increased in Figure 7D from 9.78% on day 0 to 44.6% on day 1, increasing to day 6-7 (91.6%; p=0.009). Early activation, as indicated by CD69 expression, was clearly seen in Figure 7 (E-H) at day 1 with a

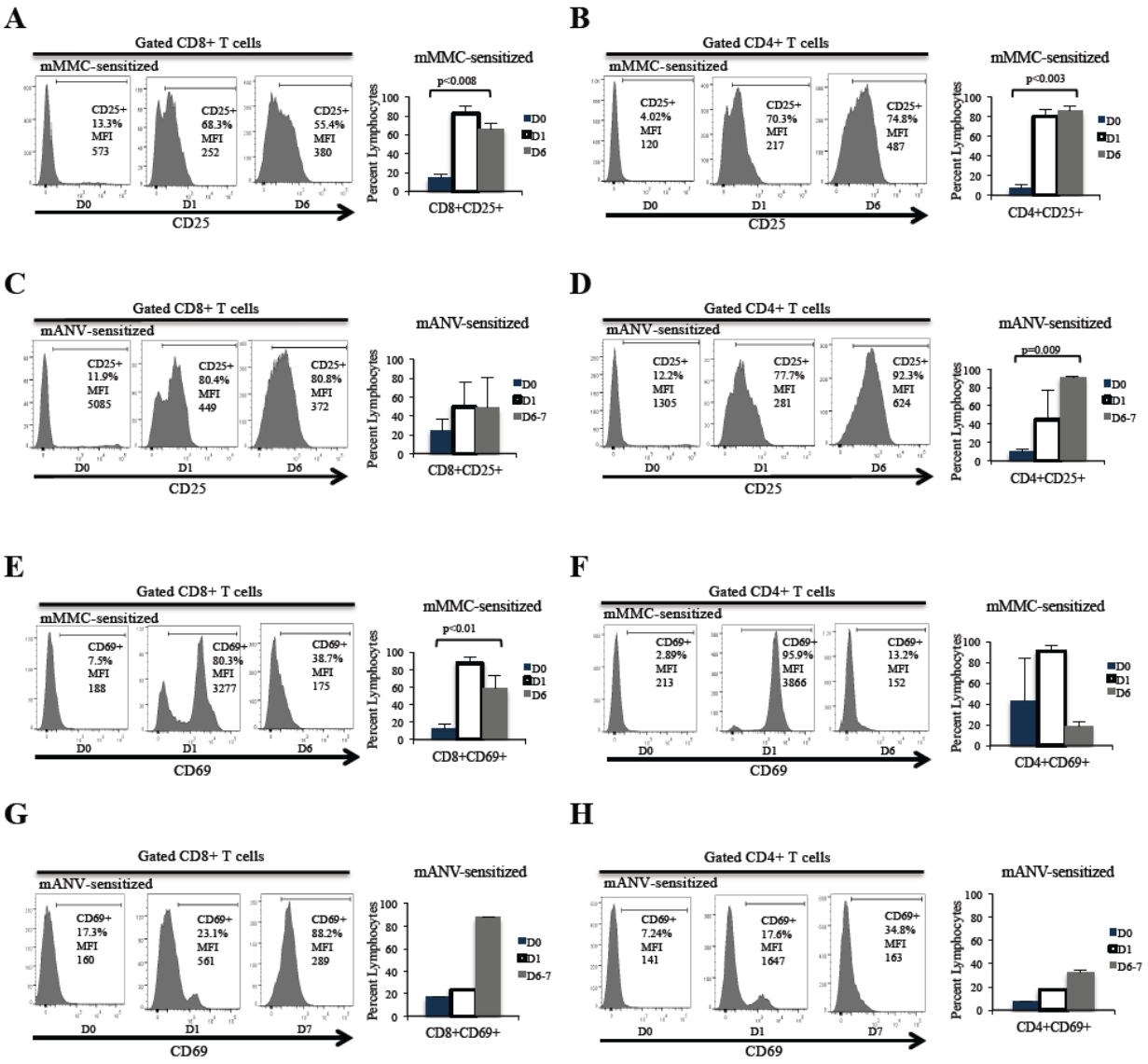

Figure 7. CD8+ and CD4+ T cells from experimental metastatic mice exhibited responsive activation by CD25 or CD69 expression during 6-7 day expansion. (A) CD8+CD25+ splenocytes from mMMC-sensitized mice (n=3) were determined by flow cytometric analysis. Representative (left panel) and averaged data shown (right panel). Significance considered for student's t-test result of $p<0.05$ (Bars indicate a significant difference between D0 vs D6). (B) CD4+CD25+ splenocytes were similarly evaluated. (C) CD8+CD25+ splenocytes from mANV-sensitized mice (n=2) were determined for comparison. (D) CD4+CD25+ splenocytes were similarly evaluated. (E) CD8+CD69+ early activated splenocytes were also determined from mMMC-sensitized mice (n=2). (F) CD4+CD69+ early-activated splenocytes were similarly evaluated. (G) CD8+CD69+ early activated splenocytes were also determined from mANV-sensitized mice (n=1 for D0,1; n=2 for D6-7). No statistical analysis was performed on incomplete data sets. (H) CD4+CD69+ early-activated splenocytes were similarly evaluated.

2- to 7-fold increase in average CD69+ cells. B/I + IL-2 induced CD69 expression on average in mMMC-sensitized CD8+ T cells (Figure 7E, 87.5% (D1); p=0.009) and CD4+ T cells (Figure 7F, 90.9% (D1)), which subsided by day 6 as expected. Expression of CD69 was not sharply detected until day 6-7 in CD8+ T cells from mANV-sensitized mice as a 5-fold increase in average CD69+ cells (Figure 7G, 87.9%), while only minimal activation was detected in CD4+ T cells (Figure 7H, 32.8%) during expansion.

Previously, we have shown that anti-tumor efficacy of reprogrammed T cells *in vivo* depended on the reprogramming and presence of activated NKT cells and NK cells (46). Tumor bearing mMMC or mANV animals were analyzed for the presence of non-T cells among the reprogrammed immune cells over the course of 6-7 day expansion (Figure 8). Notably, the larger proportion of NK cells found at day 0 and day 1, shifted to predominantly expanded NKT cells at day 6 (p=0.013) in mMMC-sensitized mice as shown in Figure 8A. By comparison, mANV-sensitized mice exhibited a similar shift of NK to NKT cells by day 6-7 in Figure 8B, while there were more NKT cells at the initial observation. Evidence of activation from day 0 to day 1 in non-T cell populations was shown in Figure 8C for splenocytes derived from mMMC-sensitized mice. NKT cells from mMMC-sensitized mice were significantly activated at day 1 with 60.7% expressing CD25 (p=0.007) and 63.5% of NK cells were activated expressing CD25 (p=0.022) at day 1 in response to B/I + IL-2. Upon closer inspection, non-T cells from mANV-sensitized mice were less responsive to B/I + IL-2 activation at day 1 (NKT25+, 16%; NK25+, 1.16%) in Figure 8D when compared to mMMC-sensitized non-T cells. Overall *ex vivo* expansion of responsive immune cells by day 6 from mMMC-sensitized mice revealed a strong presence of activated NKT cells on average (90% (D6); p=0.004) and a minor population of activated NK cells on average (40.9% (D6); p=0.043) upon reprogramming. Also, splenocytes from mANV-sensitized

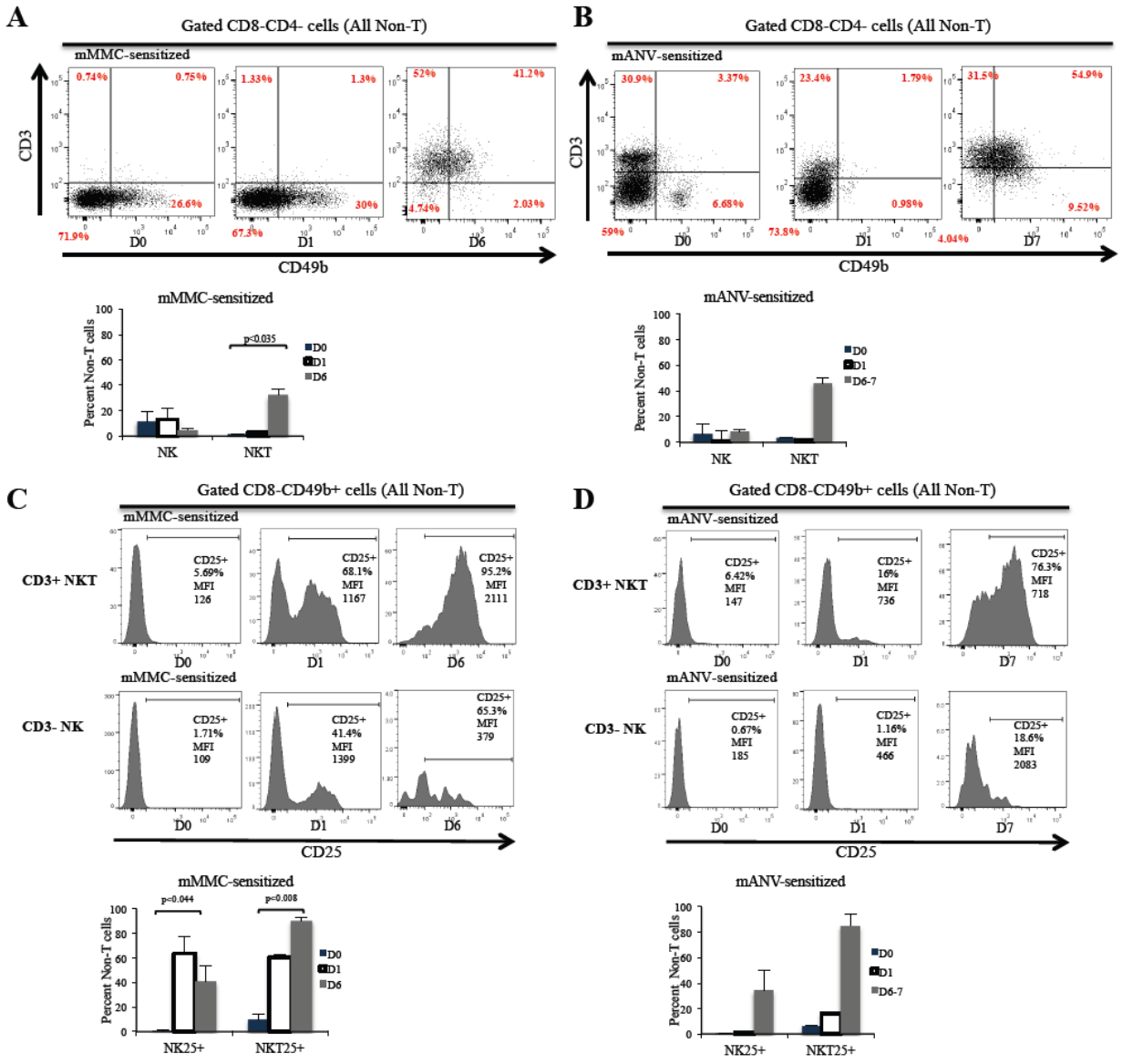

Figure 8. NK/NKT cells exhibited responsive activation during 6-7 day expansion by CD25 expression from experimental metastatic mice. (A) NKT (CD3+CD49b+) or NK cells (CD3-CD49b+) from all Non-T cells (CD8-CD4-) were assessed by flow cytometric analysis from mMMC-sensitized mice (n=3). Representative (upper panel) and averaged data shown (lower panel). Significance considered for student's t-test result of $p<0.05$ (Bars indicate a significant difference between D0 vs D6). (B) NKT (CD3+CD49b+) or NK cells (CD3-CD49b+) from all Non-T cells (CD8-CD4-) were similarly assessed from mANV-sensitized mice (n=1 for D0,1; n=2 for D6-7). No statistical analysis was performed on incomplete data sets. (C) Analysis of activated NKT (CD3+CD25+) or activated NK cells (CD3-CD25+) was performed from all Non-T cells (CD8-CD49b+) from mMMC-sensitized mice (n=3). (D) Activated NKT (CD3+CD25+) or activated NK cells (CD3-CD25+) were similarly assessed from all Non-T cells (CD8-CD49b+) from mANV-sensitized mice (n=1 for D0,1; n=2 for D6-7).

mice exhibited a similar responsive expansion of activated NKT (85.2%) and NK cells (34.5%) by day 6-7.

Tumor-specific cytotoxicity was initiated by reprogrammed T cells from mMMC-sensitized and mANV-sensitized mice

In order to determine the effectiveness of expanded splenocytes at tumor-specific killing, cytotoxicity assays were performed with reprogrammed immune cells from mMMC-sensitized or mANV-sensitized mice against each tumor-type of interest *in vitro*. Reprogrammed T cells from mMMC-sensitized mice in Figure 9A (left panel) showed some specific cytotoxicity on average against mMMC tumor (32.45% viability compared to tumor alone, 46.5%) as well as significant cross-reactivity to MMC tumor (40.65% viability compared to 59.1%), ANV tumor (54% viability compared to 82.8%) and mANV tumor (76.3% viability compared to 83.5%). The average normalized viability of tumors + T cells from mMMC-sensitized mice compared to each type of tumor was plotted (right panel) for cytotoxic effect, revealing notable cross-reactivity against MMC ($p=0.036$), ANV ($p=0.041$) and mANV ($p=0.035$). There was some variation present shown by standard error bars between mMMC + T cell samples, accounting for the lack of statistical significance despite a similar decreasing trend in tumor viability compared to other tumors treated with reprogrammed T cells. Also, the small sample size ($n=2$) undertaken for the pilot study to show cytotoxic tumor killing limits the power of the assay for drawing conclusions. For indirect study of variations in tumor-killing functions of reprogrammed cells that may be associated with activation-induced T cell death (AICD) resulting from tumor co-culture, viability of CD3+ T cells was evaluated in the presence or absence of the tumor cells *in vitro*. Activation-

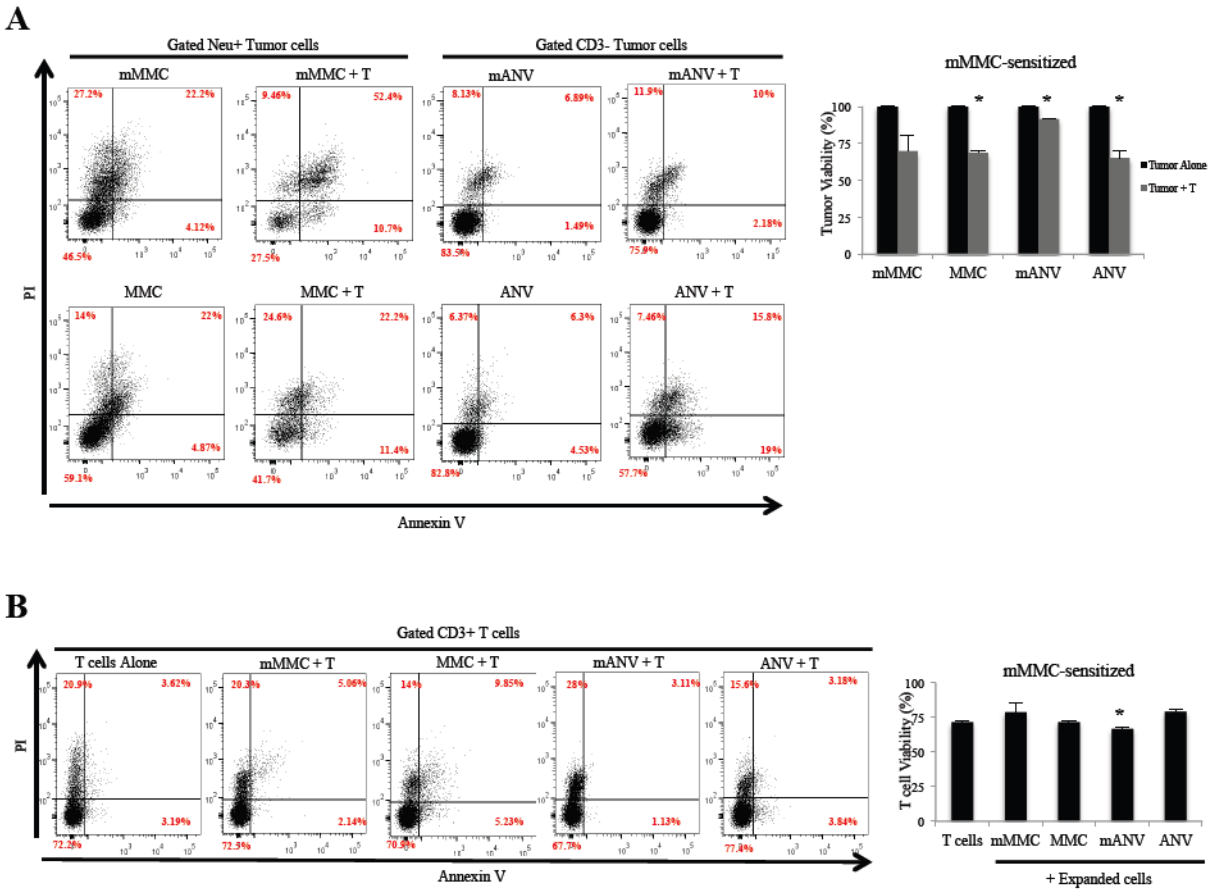

Figure 9. Average tumor-specific cytotoxicity and activation-induced cell death (AICD) of expanded splenocytes was determined from mMMC-sensitized mice cultured 48 hours with tumor (n=2). (A) Specific (mMMC + T cells vs. mMMC alone) and cross-reactive cytotoxicity (against MMC, mANV and ANV tumors) was determined by viability assay (Annexin V vs. PI) with flow cytometric analysis (Gating: neu+ or CD3- tumors). Representative data (left panel) and average normalized viability (right panel) was plotted from each tumor alone compared to each tumor + T cells. Significance (*) considered for student's t-test result of $p < 0.05$. (B) T cell AICD was analyzed from tumor (mMMC, MMC, mANV and ANV) co-cultures with T cells resulting from immune cell engagement compared with T cells alone (20 U/mL IL-2; Gating: CD3+ T) by changes in percent viability. Representative data (left panel) and average T cell AICD (right panel) was plotted.

induced cell death from mMMC-sensitized mice towards mMMC, MMC or ANV in Figure 9B was within 8% of control. Apart from AICD due to co-culture with mANV ($p=0.028$), any average reported change from control in Figure 9B was most likely due to assay variation.

By comparison, reprogrammed T cells from a mANV-sensitized mouse in Figure 10A (left panel) showed specific cytotoxicity against mANV (43.8% viability compared to tumor alone, 87.8%) and cross-reactivity against ANV (46.1% viability compared to 88.3%) as well as against neu+ MMC (40.7% viability compared to 48.3%). Normalized viability plotted of tumors + T cells from one mANV-sensitized mouse had a cytotoxic effect of up to 50% compared to each type of tumor in Figure 10A (right panel). The cytotoxic effect observed from mANV-sensitized T cells was greater than that observed from mMMC-sensitized T cells, which conflicts with the immunogenicity indicated by earlier IFN-γ production in response to mMMC tumor. Different gating strategies were employed for comparison during optimization in assessing the cytotoxic tumor-killing function of the reprogrammed T cells against MMC (CD3- cells vs. neu+ cells). When gating on intact neu+ cells, a difference in percent tumor viability (~10%) was noted between gating on CD3- cells, but the neu+ gating strategy was preferred for overall cell specificity for MMC or mMMC tumor cells. Also, all values of T cell AICD against the three tumors plotted in Figure 10B (right panel) were less than 9% difference from control, likely as assay variation.

Unlike stable mANV, stem-like mMMC exhibited reversible neu-expression upon s.c. challenge due to tumor site change

In order to determine whether any phenotypic changes in mMMC or mANV during lung

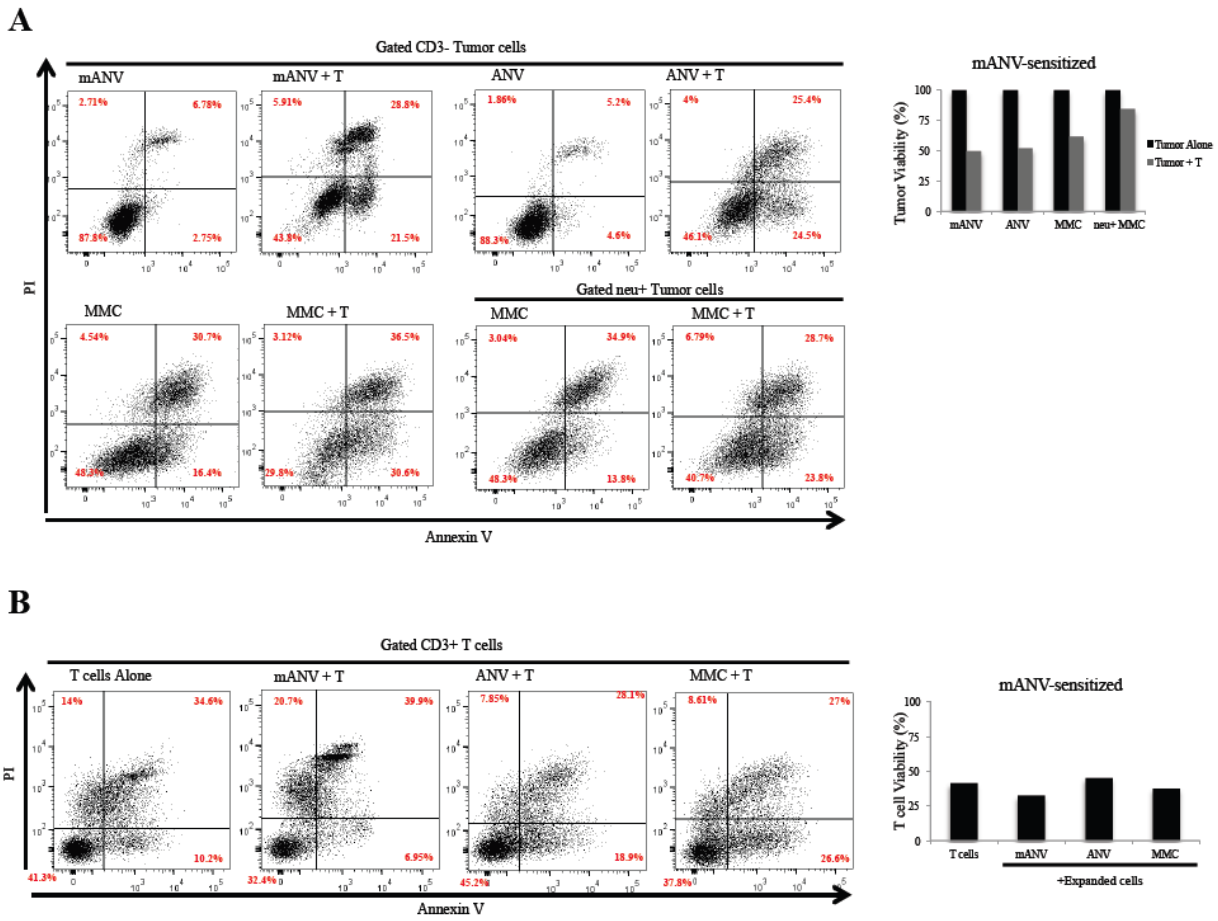

Figure 10. Tumor-specific cytotoxicity and activation-induced cell death (AICD) of expanded splenocytes was determined from one mANV-sensitized mouse cultured 48 hours with tumor (n=1). (A) Specific (mANV + T cells vs. mANV alone) and cross-reactive cytotoxicity (against ANV and MMC tumors) was determined by viability assay (Annexin vs. PI) using flow cytometric analysis (Gating: neu+ or CD3- tumor vs. SSC). Representative (left panel) and normalized viability data (right panel) was plotted from each tumor alone compared to each tumor + T cells. (B) T cell AICD was analyzed from tumor (mANV, ANV and MMC) co-cultures with T cells resulting from immune cell engagement compared with T cells alone (20 U/mL IL-2; Gating: CD3+ T). Representative data (left panel) and total T cell viability (right panel) was plotted.

metastasis remain stable or may be reversible upon the influence of tumor site, FVBN202 mice were inoculated by subcutaneous (s.c.) challenge with mMMC and/or mANV in the groin region. The purpose of simultaneous contralateral challenge with mMMC and mANV highlighted either if there were phenotypic changes exerted on the tumor cells by altering the tumor site, confirming TME crosstalk if the changes were noted in both tumors, or if the tumors were exerting phenotypic changes on each other, confirmed by subsequent separate tumor challenges as necessary. As shown in Figure 11A, mMMC retained a stem-like phenotype (CD44+CD24-, 73.4%) indicating a stable change while exhibiting a novel loss of neu-expression (neu+, 32.4-51.5% s.c. instead of 98.1-99.3 i.v.) in response to tumor microenvironment (TME) change in a tissue-specific manner. A stable expression of the neu-protein and stem-like phenotypic markers was exhibited by mANV upon s.c. challenge, indicating phenotypic stability in different tumor microenvironments. These data suggest that relapsing ANV was more stable than primary MMC upon changes in the TME during and following metastasis. Compared to MMC primary cells, neu+ metastatic tumor cells are irrevocably changed in stem-ness by susceptibility to tissue-specific TME influence.

Tumorigenicity of metastatic tumor cell lines was increased *in vivo*

In order to determine the tumorigenicity of mMMC and mANV by comparison to primary cells, FVBN202 mice were challenged s.c. with mMMC, mANV and MMC. Surprisingly, tumorigenicity of the metastatic tumor cells upon s.c. injection of mMMC and mANV on contralateral sides of the same mouse (Figure 11B, left panel) or separately inoculated in different mice (Figure 11B, right panel) conflicts with the earlier proliferation data *in vitro*

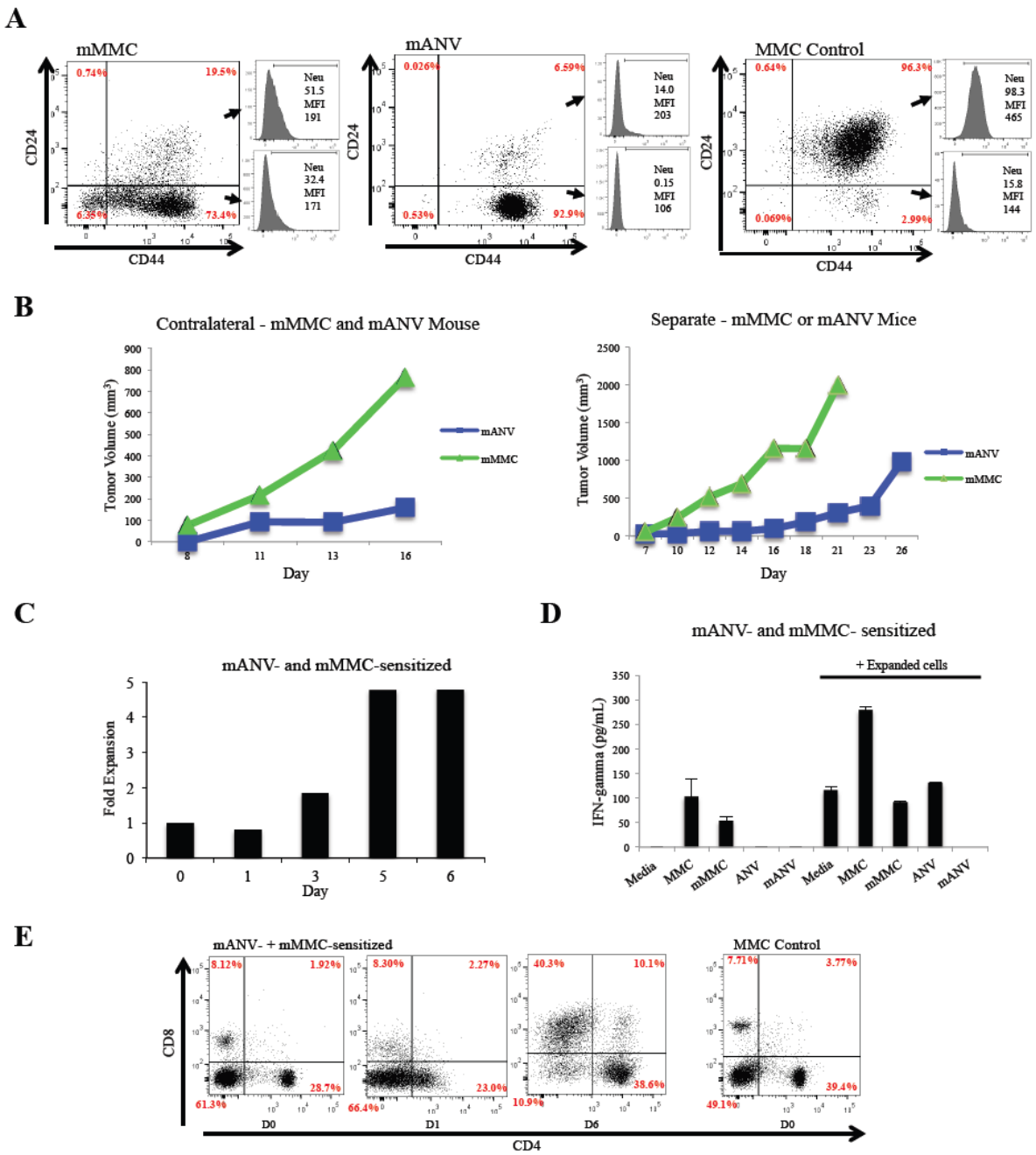

Figure 11. FVBN202 mice s.c. challenged with metastatic cells were investigated for novel TME influence on stemness, tumorigenicity, expansive capability and IFN-γ production. (A) Tissue-specific stem-like characteristics with neu-expression were evaluated by flow cytometric analysis following separate s.c. challenges with mMMC or mANV compared to MMC control. (B) Tumorigenicity of lung metastatic cells reinjected subcutaneously was measured by changes in tumor volume over time (n=1); mice received both, mMMC and mANV on contralateral sides (left plot) confirmed by subsequent separate mMMC or mANV challenges (right plot); tumor burden was measured by digital calipers. (C) Fold expansion of splenocytes was quantified from mANV and mMMC s.c. contralaterally-challenged mouse (n=1). (D) IFN-γ production was determined by ELISA of supernatants from mANV- and mMMC-sensitized splenocyte co-culture with tumors of interest (n=1). Duplicate wells were averaged. (E) CD8+ and CD4+ splenocyte population expansive capabilities were evaluated from mANV and mMMC s.c. contralaterally-challenged mouse, compared to baseline MMC Control.

(Figure 1C). Animals inoculated with mMMC showed a greater tumor burden than those inoculated with mANV tumor cells at 16 days after challenge (left panel: 750 mm^3 vs. 150 mm^3; right panel: 1150 mm^3 vs. 100 mm^3, respectively). These data are in agreement with the earlier significant differences in time for lung metastatic disease affecting moribundity to develop in mMMC-bearing mice (23.6 days) versus mANV-bearing mice (28.5 days), requiring sacrifice (Figure 1B). Further study with a more advanced invasion model would be required to determine whether the lower tumorigenicity of mANV may be because of a higher invasiveness *in vivo* that results in rapid tumor migration to distant sites parallel to primary tumor growth that would be poorly assessed by the current assays available for study, as previously noted above.

Tumor-reactive splenocyte expansion and reprogramming efficacy was unaffected by change in mMMC or mANV tumor growth site while IFN-γ production and MDSC levels were reduced

Since our previous findings have shown mMMC to be susceptible to TME influence upon s.c. challenge (above), the effect of changing tumor site following metastasis was briefly investigated for any downstream effects to the elicited anti-tumor immune response. Despite strong expansion (4.5-fold, day 5-6) from a mouse s.c. challenged with mMMC and mANV on contralateral sides (Figure 11C), a weak level of immunogenicity was indicated by IFN-γ production (average, ≤300 pg/mL) from reprogrammed splenocytes co-cultured with tumor (Figure 11D) when compared to earlier results (Figure 5A-D). A 5-fold expansion of CD8+ lymphocytes was noted by day 6 (40.3%) from day 0 (8.12%) shown in Figure 11E. Following a change in tumor localization site of mMMC or mANV, MDSC levels in FVBN202 mice s.c. challenged with mMMC and/or mANV (Figure 12) were intermediate compared to a mouse s.c.

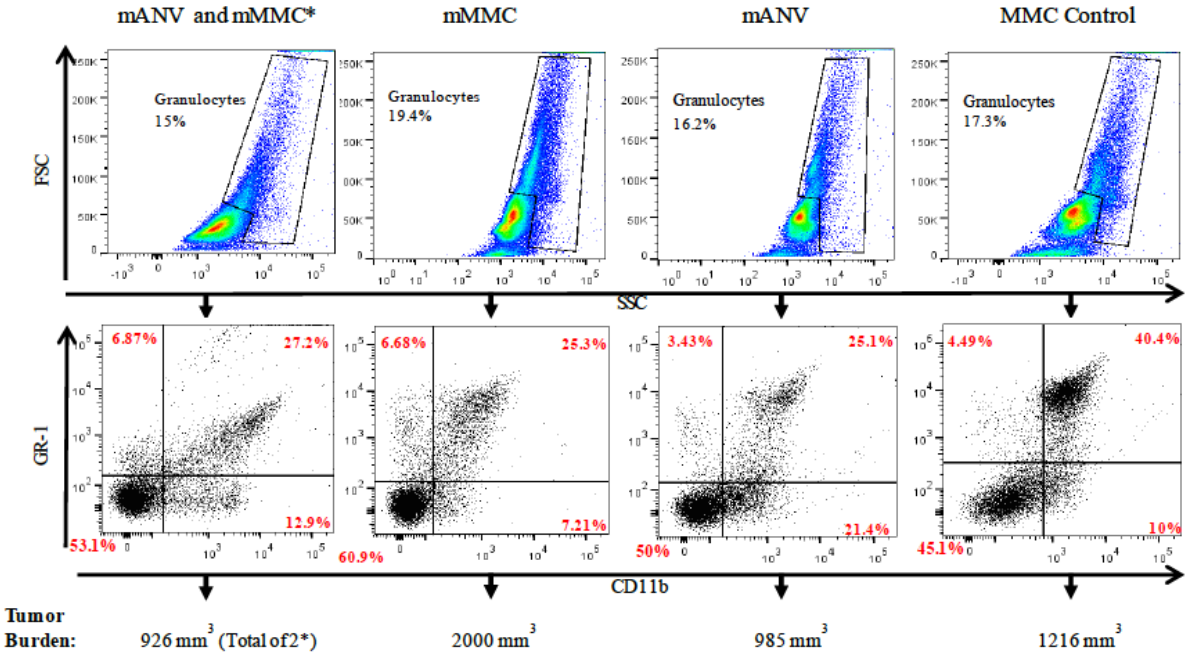

Figure 12. Splenic MDSC accumulation was not increased from TME influence in s.c. metastatic tumor-challenged mice compared to MMC. FVBN202 mice were s.c. challenged with mMMC, mANV, Both or MMC Control tumor cells (n=1). MDSCs were represented by GR-1+CD11b+ cells gated on percent granulocytes during flow cytometric analysis. *Two tumors were tracked in the mANV and mMMC s.c. contralaterally-challenged mouse.

challenged with control MMC and the previously described lung metastatic mice (Figure 4A & 4B), indicating tissue-specific effects on MDSC trafficking regardless of tumor burden.

In order to determine whether localization of mMMC or mANV in the groin region s.c. may also result in a different pattern of responses from immune cells to *ex vivo* reprogramming, splenocytes from a FVBN202 mouse s.c. challenged contralaterally with mANV and mMMC were examined. Similar trends of reprogramming as reported above in the reduction of CD62L+ T cells (including CD44-CD62L+ naïve T cells (T_N)) along with the enhancement of CD44+CD62L- effector T cells (T_E) following B/I + IL-2 treatment were observed from day 0 to day 1 in Figure 13A. Reprogramming towards a T_{CM} phenotype was still seen from day 0 to day 6 in CD8+ T cells (4.3% vs. 64.4%) or CD4+ T cells (2.6% vs. 59.6%) despite tumor site change (Figure 13A). The memory lymphocyte phenotype in the s.c. contralaterally-challenged mANV and mMMC mouse of a lower T_{EM} presence and increased T_N presence was opposite the MMC control mouse (shown at right of figure) measured at baseline (D0). A similar responsive activation status at day 1 was noted in the mANV and mMMC s.c. contralaterally-challenged mouse (Figure 13B) by CD8+CD25+ (9-fold) or CD4+CD25+ expression (21-fold) and CD8+CD69+ (4.5-fold) or CD4+CD69+ expression (6.5-fold) as previously discussed for experimental metastatic mice (Figure 7A-H). Notably, a robust activated NK cell presence was found in Figure 13C among the reprogrammed splenocytes of the s.c. contralaterally-challenged mANV and mMMC mouse by day 6 of expansion (NK, 11 or 13.7% by different gating strategies) after changes in tumor site, when compared to the earlier described metastatic mice (Figure 8). However, a similar activated NKT cell presence at day 6 (NKT25+ 94.9%) was found in the s.c. contralaterally-challenged mANV and mMMC mouse following expansion. The expanded activated lymphocyte and non-T cell populations from the s.c. contralaterally-

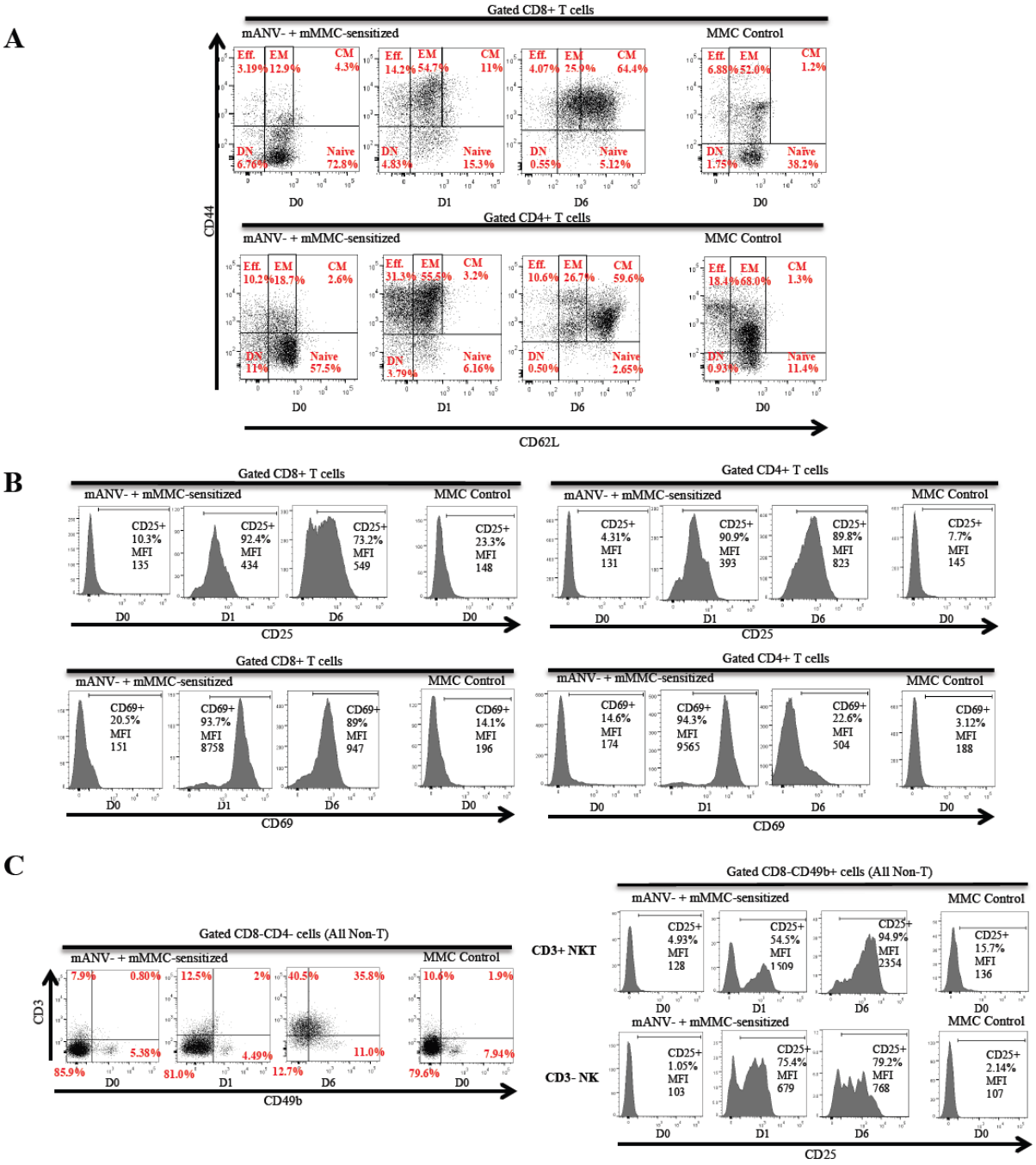

Figure 13. CD8+ or CD4+ memory splenocytes or Non-T cells showed responsive activation during 6-day expansion in mice s.c. challenged with mANV and mMMC or MMC. (A) CD8+ (Above) or CD4+ (Below) Effector, Effector Memory, Central Memory, Naiive and Double Negative (DN) splenocyte phenotypes were determined by flow cytometric analysis in comparison to MMC control at baseline (D0). (B) CD8+CD25+ (upper left panel) or CD4+CD25+ activated splenocytes (upper right panel) and CD8+ CD69+ (lower left panel) or CD4+CD69+ early-activated splenocytes (lower right panel) were also evaluated in comparison to MMC at baseline. (C) NKT (CD3+CD49b+) or NK cells (CD3-CD49b+) from all Non-T cells (CD8-CD4-) were analyzed compared to MMC at baseline (left panel). Activated NKT (CD3+CD25+) or activated NK cells (CD3-CD25+) from all Non-T cells (CD8-CD49b+) were also evaluated (right panel).

challenged mANV and mMMC mouse in comparison to the MMC control mouse (shown at right of figures) confirmed a relatively normal baseline immune response to the established metastatic tumor cells inoculated in a different tumor site.

Tumor-specific and cross-reactive cytotoxicity was initiated by reprogrammed T cells despite TME influences following s.c. contralateral challenge with mMMC and mANV

In order to determine the efficacy of reprogrammed splenocytes at tumor-specific killing from a FVBN202 mouse s.c. challenged contralaterally with mANV and mMMC, tumor-specific and cross-reactive cytotoxicity was assessed from co-culture of expanded splenocytes with the four tumors of interest. Reprogrammed T cells from the mANV and mMMC s.c. mouse show specific and cross-reactive cytotoxicity against the tumors *in vitro* (Figure 14A). A strong specific cytotoxic effect was exhibited by viability drop from 45.2% to 6.14% when comparing mMMC tumor alone to mMMC + T cells, respectively. Figure 14A also depicted the weakest cytotoxic effect by a viability drop from 80.1% to 53.3% when comparing mANV tumor alone to mANV + T cells, respectively. There was evidence of a cross-reactive cytotoxic effect from reprogrammed T cells on ANV (31.3% viability compared to tumor alone, 73.3%) and MMC (15.5% viability compared to tumor alone, 51.9%). Normalized viability data showed the previous spectral trends of specific and cross-reactive cytotoxicity upon T cell co-culture with the respective tumors of interest when compared to tumor alone. Tumor viability of mMMC by trypan blue exclusion was regularly higher than 80% following 48-hour growth, suggesting cell sensitivity to the processes/reagents of the Annexin/PI viability assay from repeated studies, hence the inclusion of data below 50% viability. The mMMC cells actively formed into clumps

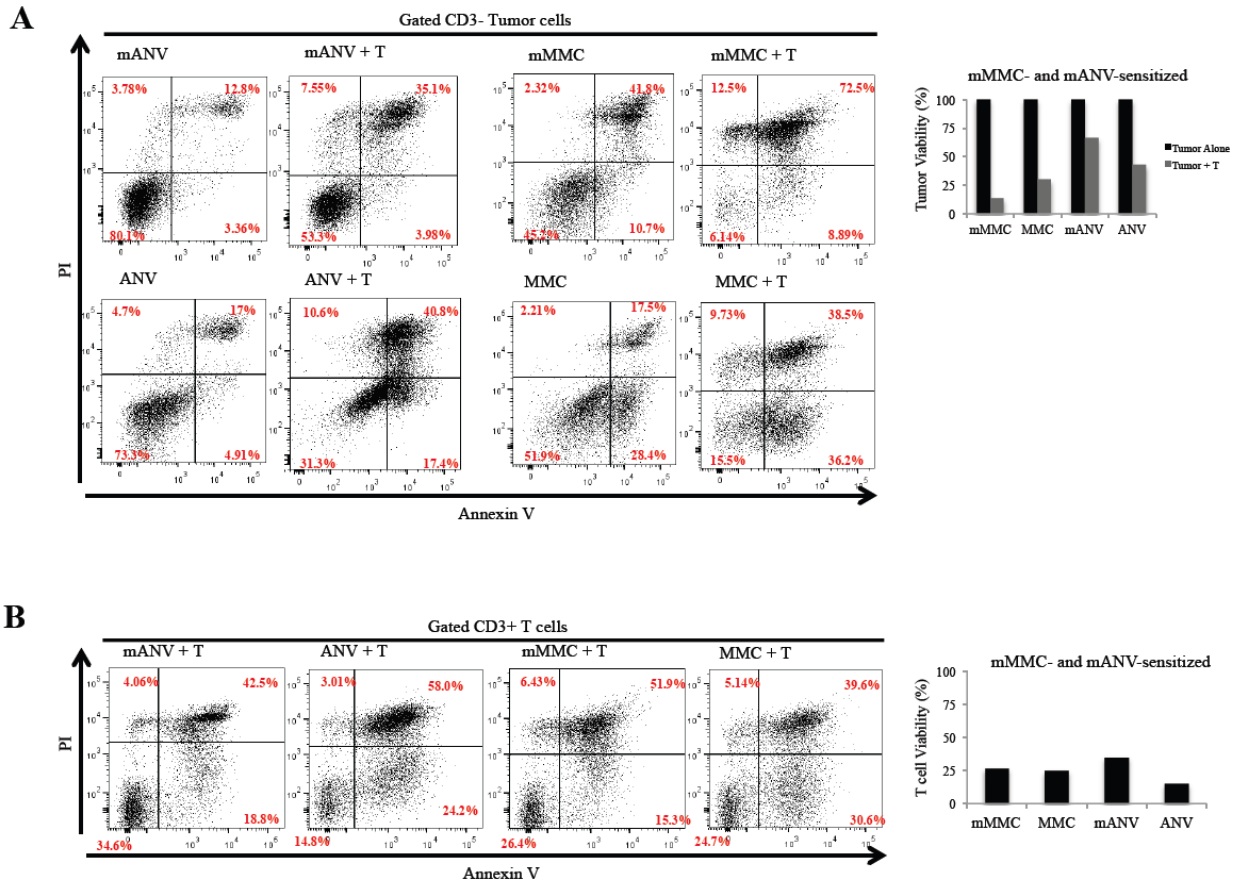

Figure 14. Tumor-specific cytotoxicity and activation-induced cell death (AICD) of expanded splenocytes was determined from s.c. contralaterally-challenged mANV and mMMC mouse. (n=1) (A) Specific (mANV + T vs. mANV alone and mMMC + T vs. mMMC alone) and cross-reactive cytotoxicity (against ANV and MMC tumors) was discerned by viability assay (Annexin vs. PI) with flow cytometric analysis (Gating: CD3- tumor vs. SSC). Representative data (left panel) and normalized viability (right panel) was plotted from each tumor alone compared to each tumor + T cells. (B) T cell AICD from tumor (mANV, ANV, mMMC and MMC) co-culture was analyzed by viability change following immune cell engagement (Gating: CD3+ T cells). Representative data (left panel) and total T cell viability (right panel) was plotted.

in suspension that were nearly impossible to disaggregate effectively through repeat pipetting or gentle vortexing without employing trypsin or EDTA. The clumped mMMC cells may have become sheared during flow analysis affecting the previous viability assay outcomes, as the sheath was designed for the passage of single cells. Further, AICD was again indirectly studied in search of variations to the tumor-killing functions of reprogrammed splenocytes co-cultured with tumor by comparison among the four tumor types of interest. AICD data (Figure 14B) suggested that the lowest amount of CD3+ T cell engagement (inversely, the highest viability) with tumor was seen with mANV (34.6%) consistent with viability loss data and the most AICD seen with ANV (14.8%).

Discussion

The efficacy of *ex vivo* expansion and reprogramming of tumor-reactive immune cells from mMMC- and/or mANV-sensitized mice was determined along with any phenotypic changes in tumors due to metastasis or TME influences (Table 1). Two cell lines were established following experimental metastasis with either MMC or ANV in FVBN202 mice. mMMC exhibited a higher macrometastatic tumor-initiating capability than mANV in the lungs while mANV exhibited higher proliferation *in vitro* than mMMC. Each metastatic cell line, mMMC or mANV, exhibited higher proliferation rates than their primary tumor counterparts, MMC or ANV, respectively, despite showing similar overall morphology. CD44+CD24-/low stem-like phenotype was acquired with enhanced neu-expression in mMMC during lung metastasis while stem-like mANV exhibited a stable lack of neu-expression. ANV invasiveness remained stable following metastatic cascade while MMC exhibited poor or very low invasiveness without effect from metastasis. MDSC levels were not increased in experimental metastatic mice nor was splenomegaly observed. Splenocytes were successfully expanded on average from mMMC-sensitized mice and/or mANV-sensitized mice using B/I + γ-c cytokines over 6-7 days. CD8+ and CD4+ splenocytes were expanded in mMMC- or mANV-sensitized mice. The 6-7 day expansions resulted in tumor-specific and cross-reactive IFN-γ production from reprogrammed splenocytes in mMMC- or mANV-sensitized mice. *Ex vivo* expansion and reprogramming was successful due to the downregulation of CD62L expression simultaneously with an increase in effector T cells at day 1, signs of responsive activation by CD25 or CD69

Table 1. Summary of key findings

- **Experimental lung metastasis resulted in the establishment of two cell lines, mMMC and mANV**
- **mMMC exhibited a higher macrometastatic tumor-initiating capability than mANV in the lungs**
- **mANV exhibited a higher proliferative rate than mMMC *in vitro***
- **Metastasis directly increased the proliferative rates of mMMC and mANV over MMC or ANV *in vitro***
- **Metastasis induced CD44+CD24-/low stemness phenotype with enhanced neu-expression in mMMC**
- **mANV retained a stable stemness phenotype and lack of neu expression during metastasis**
- **Metastasis failed to effect the invasiveness pattern of invasive ANV or non-invasive MMC *in vitro***
- **MDSC levels were not increased in lung metastatic mice bearing mMMC or mANV**
- **CD8+ and CD4+ splenocyte expansion was successful from lung metastatic mice using B/I + γ-c cytokines**
- **Tumor-specific and cross-reactive IFN-γ production was observed in mMMC- or mANV-sensitized mice**
- **Successful reprogramming of splenocytes was observed from mMMC- or mANV-sensitized mice**
- **Responsive activation was indicated by CD25 or CD69 expression in mMMC- or mANV-sensitized splenocytes**
- **Central memory T cells and activated NK/NKT cells were differentiated from mMMC- or mANV-sensitized mice**
- **Tumor-specific and cross-reactive cytotoxicity was observed from mMMC- or mANV-sensitized splenocytes**
- **Tumor site change effected a reversal in neu-expression without an effect on stemness in mMMC**
- **Tumorigenicity was increased for mMMC over mANV *in vivo* upon tumor site change**
- **Tumor-reactive splenocyte expansion and reprogramming was unaffected by mMMC and mANV tumor site change**
- **Tumor site change of mMMC and mANV reduced IFN-γ production and MDSC levels compared to primary tumors**
- **Tumor site change of mMMC and mANV did not alter the initiation of a positive anti-tumor cytotoxic response**
- **We propose the prophylactic use of ACT against metastatic or recurrent breast cancer after conventional treatment**

expression at day 1 and the phenotypic differentiation of central memory T cells with activated NK/NKT cells by day 6 from mMMC- or mANV-sensitized mice. Tumor-specific and cross-reactive cytotoxicity was observed from splenocytes expanded from mMMC- or mANV-sensitized mice. The contributions of tumor site on metastatic disease were determined in mice s.c. challenged with mANV, mMMC or both contralaterally. Neu-expression was flexibly reversed in mMMC s.c. challenged mouse while a stable phenotype was observed in mANV (lack of neu) or MMC control (neu-overexpressing) s.c. challenged mice. Tumorigenicity was increased for mMMC over mANV *in vivo* in mice s.c. challenged with mANV, mMMC or both contralaterally. Further, tumor-reactive splenocyte expansion and reprogramming efficacy was unaffected by change in mMMC and mANV tumor growth site while IFN-γ production and MDSC levels were reduced, compared to primary tumors. Finally, tumor-specific and cross-reactive cytotoxicity was initiated by reprogrammed immune cells despite TME influences following s.c. contralateral challenge with mMMC and mANV.

mMMC and mANV were studied following experimental metastasis by tail-vein injection for their phenotypic changes in disease progression, growth character, stemness changes, proliferation rate, invasiveness and suppressive cell recruitment. By comparison to their primary counterparts, the metastatic cells revealed some very interesting phenotypic changes that correlate with tissue-tropism and common metastasis-induced mesenchymal or epithelial changes (11). Macrometastatic disease formed in the lungs of mMMC-sensitized mice faster than mANV-sensitized mice on average. Pulmonary metastasis gave rise to established cell lines, mMMC and mANV, that proliferated faster *in vitro* compared to the original MMC and ANV. Our group previously showed a higher proliferative capacity in ANV compared to MMC, which was conserved by our experiments *in vitro* following experimental metastasis (53). The enhanced

level of growth factors and compatibility of the growth surface *in vitro* have been implicated in differences in cellular proliferative capacity, but further molecular studies would be required to remove speculation in differences between the two differing tumor microenvironments.

Growth character was similar following metastasis for mMMC and mANV compared to their primary tumor counterparts, yet mMMC showed a high degree of aggregation when in suspension that required extensive chemical or mechanical disaggregation. This alteration to cell adhesion is consistent with reductions in gene expression responsible for tight junctions or intercellular adhesion (e.g., E-cadherin) following the metastatic cascade as previously reported in mammary carcinoma (23, 63-66). The suggested changes in tumor aggregation have been linked with changes in tumor initiation and self-renewal associated with the epithelial to mesenchymal transition (EMT) portion of the metastatic cascade when tested for mammosphere formation (12, 67-69). ANV and mANV exhibited a spindle-like morphology characteristic of mesenchymal cells that in this instance may have undergone EMT during initial relapse (12, 23, 24, 67-69). As expected, mANV was invasive and migratory through Matrigel following metastasis, similar to ANV, as previously shown by pathology (7). However, mMMC was not invasive following metastatic cascade like MMC, showing no tumor cell-derived change in invasion. Recently, tumor dissemination has been explored from metastatic and non-metastatic breast carcinomas influenced by tumor-associated macrophages (TAMs) or neoangiogenesis as potent inducers of metastasis (27, 70, 71). These prospects of metastatic initiation via TAMs and angiogenic means are probable in our current experimental metastatic model due to the previously reported production of MCP-1/CCL2 (monocyte/macrophage chemoattractant) and VEGF (angiogenic soluble factor) in mouse mammary carcinoma (48).

Previously the stem-like phenotype, CD44+CD24-/low, was characterized in mammary carcinoma to show an increased tumorigenicity (14, 15), but it has also been associated with increases in potential tumor initiation and drug/radiation resistance (16-18). Upon lung metastasis, a stem-like phenotype of CD44+CD24- was induced in mMMC from the original CD44+CD24+ MMC, while the stemness of primary ANV was retained in mANV. Neu-protein expression increased following metastasis with MMC, but no change was seen with relapsing ANV, indicating phenotypic stability. The simultaneous loss of CD24 expression and upregulation of neu expression indicates flexibility in mMMC to the metastatic process that is not solely selection of surviving clones which may be due to epigenetic modifications during metastasis (72). The fluctuation in neu expression has previously been evaluated in response to various treatments by our group (53). However, this was the first instance that conclusively showed two changes in the original MMC population, opposite in trend yet similar in the nature of suggested epigenetic modification. If the trend were Darwinian selection, clonal enrichment would be selected for during metastasis from the CD24- population with low neu expression, which was not the case. Bisulfite sequencing would be required to confirm any changes to methylation states, but based on previous work by our group, the stability of ANV is most likely due to the higher degree of methylation (gene silencing) present when compared to MMC at the MMTV promoter (53). The hypomethylation of MMC previously allowed for increased expression of neu, but this lower level of genetic stability could also lead to the epigenetic loss of CD24 during metastasis or relapse. Many groups have observed epigenetic changes during cancer progression, including an induced state of hypermethylation of multiple proximal promoters to stemness-related genes, drastically altering the phenotypes of adult human cancers (72). The proposed epigenetic changes in response to the TME may be the means for initial

relapse of ANV to an alternate site with less tissue-specific neu expression, affecting its growth pattern towards temporary dormancy while experiencing immune pressure to survive. Previous connections to immune regulation of breast cancer cells showed changes in HER2/neu+ expression as a form of immune escape (23, 53) that could be flexible in response to tissue-specific HER2/neu+ expression when involved in crosstalk with various tissues, including the compatible HER2/neu+ lungs during metastasis (73). Lung tissue also produces tumor-promoting TGF-β1 and periostin, while other cancers have been associated with pulmonary metastases due to the welcoming VEGFR1+ endothelial microenvironment and MMP9 activity from TAMs (71, 74, 75). This idea of tissue compatibility during metastasis and survival signaling at the secondary site(s), instead of required growth factors, may be key to understanding the tendency toward dormancy of disseminated cells allowing for disease recurrence 25 years later (27, 28, 75).

Our group has previously linked the release of tumor-derived soluble factors to a rise in circulating MDSC levels (48). These immunosuppressive cells have previously been linked to tumor evasion and ultimate escape (45). Reprogrammed immune cells have been effective at overcoming MDSC suppression (due to NK/NKT cells) in prophylactic adoptive transfer against primary MMC (46). Amidst mixed reports on suppression models present in metastatic breast cancer (40, 76, 77), the MDSC involvement in our metastasis model was determined. Previously, our group determined that regulatory T cells were not present following B/I + γ-c cytokine expansion based on suppression functions measured *in vitro* (58), while MDSC suppression has been characterized in our FVBN202 mouse model (45, 48). MDSC levels were not increased in mice bearing lung metastases, suggesting an altered phenotype of soluble factor (GM-CSF) release from mMMC or mANV as a result of metastatic cascade (48).

Splenocytes from mMMC-sensitized or mANV-sensitized mice were successfully expanded and shown to be tumor-reactive by IFN-γ production following a characteristic drop in numbers from reprogramming with B/I + γ-c. The successful expansion of tumor-reactive splenocytes from mMMC-sensitized or mANV-sensitized mice was evident from the CD8+ and CD4+ T cell increases over 6-7 day expansion, as seen before by our group (46). The potential technical issue for one mouse, indicated by an unexpected viability fluctuation and variation shown by standard error, explains the lack of statistical significance at this early stage in the pilot study despite the observed increasing trends of average CD8+ or CD4+ T cells from mANV-sensitized mice during expansion. It is likely the increasing trends would be reinforced upon further repeats, as supported by the relatively similar IFN-γ production among mMMC- or mANV-sensitized mice. The cross-reactive nature of IFN-γ production from expanded mMMC- or mANV-sensitized immune cells suggests the greater immunogenicity associated with the neu+ MMC cells when compared with the antigen-negative variant (ANV). Interestingly, despite the antigen difference, mice sensitized with opposite tumor cell types retained reactivity against both tumor types and in the case of mANV-sensitized mice, produced a stronger IFN-γ response against opposite tumor, neu+ MMC. Again, with further repeats we would expect reinforced trends of tumor-specific and cross-reactive IFN-γ production following metastatic cascade as the study progresses. Notably, the nature of tumor-specific IFN-γ production along with cross-reactivity against opposite tumors elicited during the anti-tumor immune response may have ramifications in enhanced immune cell access to circulating tumor cells during the metastatic cascade through the vasculature, but it also shows that certain cell epitope signatures may not be lost during neu-antigen loss under immune pressure when considering the effective priming of an anti-tumor response towards mMMC or mANV (26, 55, 78).

Reprogramming with B/I + IL-2 resulted in the downregulation of CD62L expression, including the characteristic reduction of T_N cells, along with the strong increase in T_E cells following treatment in either mMMC- or mANV-sensitized mice. Further evidence of successful reprogramming was shown in the activation events indicated by CD25 or CD69 expression in mMMC-sensitized mice and later seen in mANV-sensitized mice. Phenotypic differentiation of splenocytes into T_{CM} cells following expansion was observed in all lung metastatic mice. Previous work by our group has shown that AIT performed with the separate T cell subtypes suggests a synergy for effective protection against tumor, lost when subtypes were separately tested (46), but the T_{CM} cells have been reported to confer the greatest long-term anti-tumor protection (79-81). Further, the NK/NKT cell populations were investigated for their contribution to the anti-tumor immune response and to overcoming immunosuppression (46). An increase in NK cells was seen in response to B/I, but the population had decreased by the end of expansion, while a strong increase in NKT cells was observed throughout expansion. Activation was indicated in both NK and NKT cells, with emphasis on the latter. The importance of activated NKT cells during an effective anti-tumor response has recently been shown to be an NKG2D-dependent interaction (manuscript submitted). Apart from a general reduction in effector, effector memory, and NK cells following expansion, the trends in successful reprogramming and phenotypic differentiation examined in our experimental metastatic model follow our earlier work with MMC injected s.c. in FVBN202 mice (46).

Tumor-reactive splenocytes expanded from mMMC-sensitized and mANV-sensitized mice caused specific and cross-reactive cytotoxicity upon 48-hour co-culture with the tumors of interest. Tumor-specific and cross-reactive cytotoxicity in mMMC-sensitized mice was elicited roughly equally against mMMC (n.s.), MMC, and ANV, while a weaker significant cross-

reactive cytotoxicity was elicited against mANV tumors. Specific cytotoxicity in a mANV-sensitized mouse was elicited against mANV and ANV while less cross-reactive cytotoxicity was elicited against MMC tumors. Specific and cross-reactive tumor cytotoxicity confirms the idea that *ex vivo* reprogrammed splenocytes from mMMC-sensitized and mANV-sensitized mice can effectively target and destroy tumor *in vitro*. Another immune evasive technique recently proposed is the Fas-counterattack where a tumor may display Fas-L to induce apoptosis in T lymphocyte populations similar to normal T cell population regulation (82). Activation-induced cell death (AICD) was monitored for variations of reprogrammed cell activity during tumor co-culture. The level of AICD present in both mMMC-sensitized and mANV-sensitized mice were similar to control, with any reported difference within a range of 9% viability away from the control. The only significant difference in AICD found in the reprogrammed cells was from mMMC-sensitized T cells co-cultured with mANV, but based on the tumor viability of mANV, it might simply have been a case of tumors outcompeting T cells for nutrients *in vitro*. These results indicate there is not an active immune evasive technique being employed by the tumor cells following metastasis because there were no associated changes to viability between tumor/ T cell co-cultures to indicate a Fas/FasL counterattack present in our cells.

By changing the tumor site, the stability of the stem-like phenotype and neu expression found on mMMC and mANV could be investigated in response to tumor microenvironment changes. Following s.c. injection with mMMC, the stem-like phenotype was mostly retained while neu expression was downregulated in both, CD24- or CD24+ populations. After s.c. injection with mANV, the stem-like phenotype and neu expression was stable despite tumor site changes. By comparison to stable primary MMC cells injected s.c., mMMC cells were only stable for the stem-like phenotype but flexibly reversed in neu expression. The effects of the

metastatic cascade caused a stable change toward stemness in mMMC, but left mANV unchanged, possibly due to methylation differences as previously reported (53) which caused the susceptibility to change in mMMC. The dynamic process of metastasis caused more than just immune pressure as the neu expression change upon tumor site change could be explained. The pressure to survive in distant sites may be the trigger towards adopting a stem-like phenotype by epigenetic means within the same generation of cell growth due to crosstalk with the new TME following tissue-tropic metastatic homing and, recently proposed, autophagy (22).

Tumorigenicity was determined upon s.c. injection of mMMC and mANV on contralateral sides, confirmed with subsequent separate challenges of the tumors. The tumor burden resulting from mMMC was greater than from mANV, along with a faster rate of development. The change in tumorigenicity conflicted with earlier proliferation data but the time to develop the tumors s.c. was consistent with the average time for development of lung metastatic disease that affects overall health (above). The change in mANV growth *in vivo* could be explained by a greater degree of invasiveness upon metastasis if the tumor rapidly migrated away from the s.c. site of challenge, according to the parallel metastasis model (8). Alternatively, a potentially higher degree of methylation could also limit the proliferative rate of mANV similar to the original relapse event for a certain amount of time before reactivation if induced by metastatic cascade, which would correlate with the induction of stemness at initial relapse (72).

The expansion of splenocytes from a mouse s.c. contralaterally-challenged with mMMC and mANV was stronger than lung metastatic mice challenged with mMMC or mANV, most likely due to altered immune cell types trafficking to the subcutaneous tumor site or increased immune cell access to prime a response against two tumors instead of single challenge with great proximity to draining lymph nodes during dendritic cell maturation. The IFN-γ response of

reprogrammed splenocytes to the tumors when s.c. contralaterally-challenged with mMMC and mANV was lower than the response from mMMC-sensitized or mANV-sensitized splenocytes from lung metastatic mice. Further, the MDSC trafficking in s.c. contralaterally-challenged mice with mMMC and/or mANV was intermediate compared to the lower levels in mMMC-sensitized or mANV-sensitized lung metastatic mice and the levels observed in mice s.c. challenged with primary MMC, regardless of tumor burden or time after challenge. This difference in MDSC trafficking is most likely due to an altered lower expression pattern of tumor-derived soluble factors, including GMCSF, following metastasis even with the tumor site changed back to our original s.c. model (48).

Splenocytes were also phenotypically characterized from the mMMC-sensitized and mANV-sensitized s.c. contralaterally-challenged mouse for any contribution of change in tumor site on the immune response following metastasis. Similar trends were observed in the mMMC-sensitized and mANV-sensitized s.c. contralateral-challenged mouse during reprogramming. A similar downregulation of CD62L expression (including naive T cells) and an enhancement of effector T cells was exhibited following B/I treatment. Also, a robust expansion of CD8+ lymphocytes was similarly seen here. A responsive activation was similarly seen by CD25 and CD69 expression following B/I in CD8+ or CD4+ lymphocytes. Surprisingly, a larger NK presence was noted upon s.c. challenge during expansion than with mMMC-sensitized or mANV-sensitized lung metastatic mice, similar to our previous work with subcutaneous challenge. This difference in NK cell proportion expanded may be a tissue specific change upon s.c. tumor challenge. A similar level of NKT cells was observed among the different challenges and the activation of non-T cells was relatively equivalent when comparing mMMC-sensitized or mANV-sensitized lung metastatic mice to the s.c. contralaterally-challenged mouse. When

comparing the s.c. contralaterally-challenged mouse to a mouse challenged s.c. with MMC control for baseline, the immune response was relatively normal upon dual tumor challenge with the only difference being a lower effector memory and increased naive cell presence in the contralateral mouse.

In order to see if a tumor site change may affect the efficacy of reprogrammed splenocytes at tumor killing, cytotoxicity was assessed from co-culture of splenocytes from mMMC and mANV s.c. contralaterally-challenged mouse with the tumors of interest. A strong viability drop indicated specific and cross-reactive cytotoxicity against all four tumors with contralateral challenge s.c. A high degree of AICD was implied for T cells co-cultured with any of the four tumors that could confirm the expected high level of T cell engagement with tumor already described from the viability data, in addition to the strength of expansion indicated. However, the strong cytotoxic tumor killing indicated is inversely related to the IFN-γ levels reported from the contralaterally-challenged mouse. The previous difficulty with optimizing the cytotoxicity assay indicates the need for replicates to confirm any preliminary trends. Again, the level of AICD would indicate there is not an appreciable change in Fas/FasL expression as a form of immune evasion in the metastatic tumors since none of the T cell samples were significantly different than each other without a T cell control to be certain during assay optimization (82).

Despite the losses in some tumor-reactive cell types, the results of substantial T_{CM} cell and activated NKT cell expansion make a strong case for the application of adoptive cellular therapy (ACT) in metastatic or relapsed malignant disease. Our group previously showed effective primary tumor rejection in a prophylactic setting instead of therapeutic setting (46), but with our metastatic model there might be more clinical benefit from prophylactic vaccination

with tumor-reactive reprogrammed immune cells on preventing relapse or distant metastasis. This is supported by the cross-reactivity exhibited by the cytotoxicity and IFN-γ production against primary or relapsing forms of tumors upon metastasis, where the cells have not necessarily changed so much that the multi-faceted anti-tumor immune response would be evaded. The retained effective cytotoxicity against all four tumors despite a change in tumor site provides further evidence for the use of reprogrammed splenocytes as a preventive vaccine against recurrence to prolong cancer-free survival. If peripheral blood was collected from patients before conventional therapy for cryopreservation and then expanded for subsequent ACT following various treatments, the vaccination could greatly benefit the long-term anti-tumor immune response in patients, resulting in potential recurrence or metastasis prevention for some time by conferring a response against circulating or disseminated tumor cells. New drug-targeted methods of therapy for metastatic disease have focused on the many steps of the metastatic cascade for inhibition of tumor growth, the associated soluble factors (like VEGF) or affecting the tumor compatibility with the surrounding TME of the pre-metastatic niche (11). If the ACT was administered in concert with some of these targeted methods against the permissive TME, a longer distant recurrence free interval may be achieved to prolong survival through synergistic or sequential therapeutic effects.

In the context of prevention, highly effective cancer vaccines or therapeutics have not been developed since the success of prophylactic vaccination (nearly 100% efficacy) with human papillomavirus (HPV) virus-like particles in 2006, providing humoral immunity against variants known to cause cervical cancer (83). Other groups have had success in the field of cancer vaccine performance when providing T-helper peptides specific for HER2/neu extracellular domains to prime a humoral response that resulted in epitope spreading (55, 56). Recently, Sun

et al. (38) studied the clinical use of expanded activated autologous lymphocytes from the peripheral blood on metastatic breast cancer following adjuvant therapy and observed a response during 25-month period (progression free disease or stable disease) in 3 out of 4 stage IV breast cancer patients to prolong overall survival (median: 11.5 months). The metastatic breast cancer patients also showed significant increased CD8+ Cytotoxic T lymphocytes (CTL), Natural Killer (NK) and NKT cells following infusion (38). Also, Domschke et al. (37) has found that metastatic breast cancer patients with pre-existing tumor reactive bone marrow memory T cells could receive effective ACT with T cells that have been reactivated with autologous MCF7 breast cancer lysate-pulsed dendritic cells. Almost half the patients (44%) had *de novo* induction of tumor-reactive memory T cells in the peripheral blood following ACT as a positive response to immunotherapy (37). Longer survival was associated with a positive immunologic response to ACT, a prior high-level tumor-reactive bone marrow T cell population and a higher estimated number of transferred tumor-reactive T cells (37). These correlations, along with the consideration of separating stage IV patients novice to treatment from disease recurrence patients refractory to treatment (2), provide important treatment considerations for metastatic breast cancer patients moving forward. The ideas put forth by Seong and Matzinger (84) combining the Danger and Self/Nonself models, by considering the access to cryptic immunogenic epitopes induced by cellular stress, highlighted the need for the quality of the avid immune response to many antigenic targets (similar to humoral epitope spreading (55)) instead of the quantitative high-affinity immune response against a single antigen, like overexpressed neu protein. This strategy of including cryptic epitopes that have not been involved in thymic selection following danger signaling (54) may have bearing on the elicited immune reponse to metastatic tumor cells that have undergone massive changes during relapse or distant site deposition. Pioneering work

done by June and colleagues with leukemia or HIV treatments using ACT has attracted more attention to the field with an impressive level of success in responders for the induction of remission or long-term responses (85). Recently, Kumar et al. (86) investigated a prophylactic strategy with aggressive leukemia treatment using donor leukocyte infusion against recurrence to find that 25% of patients that received leukocytes in addition to stem cell therapy achieved complete remission. While the option of prophylactic use of donor-derived ACT during minimal residual disease in aggressive hematologic malignancies may not be much more useful at warding off relapse or prolonging survival than current treatment plans due to GVHD, the strategy using autologous lymphocytes may still be useful in other forms of cancer at least as an alternative in more appropriate forms of cancer for immunologic responders. The preventive use of ACT, providing *ex vivo* expanded autologous tumor-reactive immune cells comprised of innate (NK/NKT cells) and adaptive components (CD8+ central memory T cells), has not previously been proposed in metastatic or recurrent breast cancer models. When considering current metastatic breast cancer treatment modalities (5, 87-89) or the challenges to provide novel therapeutics that consider TME influence (90, 91), this new preventive strategy could be an effective form of immunotherapy at prolonging survival following surgery, radiation and/or chemotherapy. After primary tumor removal and confirmation of minimal residual disease, this prophylactic treatment may be effective at boosting the immediate innate anti-tumor immune response, skewing it towards elimination of any disseminated or circulating tumor cells, and providing a long-term adaptive memory response against recurrence. In addition, it also may fulfill a niche when other treatments initially fail (like Trastuzumab) due to refractory disease or dependent on the suppressed host immune response.

Conclusions

We have outlined the changes associated with metastasis of mouse mammary carcinoma compared to metastatic relapse of its antigen negative variant. The stable changes in the tumor cells resemble a stem-like dedifferentiation to harness the mammalian machinery employed in the deposition of normal stem cells to various tissues based on neu expression. The stem-like changes to tumor were most likely induced by epigenetic changes in mMMC instead of selective enrichment of clones. The TME has been implied to be involved in a crosstalk with the tumor cells driving the changes observed, including the rate of macrometastatic tumor initiation or tumorigenicity *in vivo*. The immunosuppressive MDSC levels were not increased in association with lung metastasis in our model, contrary to the previously described s.c. tumor site. The metastasis-derived changes also appear to be functionally beneficial to the cell survival in the lung TME or back in the s.c. TME, but the multi-antigenic signature recognized by the anti-tumor immune response was not lost against MMC or ANV. The B/I + γ-c expansion protocol effectively reprograms and phenotypically differentiates splenocytes towards activated NK/NKT cells and T_{CM} cells sensitized by mMMC or mANV, despite tumor site. These tumor-reactive splenocytes also effectively produce IFN-γ and an *in vitro* cytotoxic effect towards primary or metastatic tumor. We propose a preventive treatment strategy of *ex vivo* reprogrammed tumor-reactive immune cells that could be effectively employed to prevent the relapse or metastasis of mouse mammary carcinoma in the preclinical setting, hopefully translating to prolonged patient survival in the clinical setting, when other treatment modalities prove ineffective.

References

References

1. American Cancer Society. 2013. Breast cancer facts and figures 2011-2012. Available at: http://www.cancer.org/cancer/breastcancer/detailedguide/breast-cancer-pdf2 or http://www.cancer.org/cancer/news/expertvoices/post/2013/01/23/unlocking-the-mysteries-of-metastasis.aspx

2. Dawood, S., K. Broglio, J. Ensor, G. N. Hortobagyi, and S. H. Giordano. 2010. Survival differences among women with de novo stage IV and relapsed breast cancer. *Ann. Oncol.* 21: 2169-2174.

3. Tevaarwerk, A. J., R. J. Gray, B. P. Schneider, M. L. Smith, L. I. Wagner, J. H. Fetting, N. Davidson, L. J. Goldstein, K. D. Miller, and J. A. Sparano. 2013. Survival in patients with metastatic recurrent breast cancer after adjuvant chemotherapy: little evidence of improvement over the past 30 years. *Cancer* 119: 1140-1148.

4. Siegel, R., C. DeSantis, K. Virgo, K. Stein, A. Mariotto, T. Smith, D. Cooper, T. Gansler, C. Lerro, S. Fedewa, C. Lin, C. Leach, R. S. Cannady, H. Cho, S. Scoppa, M. Hachey, R. Kirch, A. Jemal, and E. Ward. 2012. Cancer treatment and survivorship statistics, 2012. *CA Cancer. J. Clin.* 62: 220-241.

5. Mittendorf, E. A., Y. Wu, M. Scaltriti, F. Meric-Bernstam, K. K. Hunt, S. Dawood, F. J. Esteva, A. U. Buzdar, H. Chen, S. Eksambi, G. N. Hortobagyi, J. Baselga, and A. M. Gonzalez-Angulo. 2009. Loss of HER2 amplification following trastuzumab-based neoadjuvant systemic therapy and survival outcomes. *Clin. Cancer Res.* 15: 7381-7388.

6. Banerjee, S., J. S. Reis-Filho, S. Ashley, D. Steele, A. Ashworth, S. R. Lakhani, and I. E. Smith. 2006. Basal-like breast carcinomas: clinical outcome and response to chemotherapy. *J. Clin. Pathol.* 59: 729-735.

7. Idowu, M. O., M. Kmieciak, C. Dumur, R. S. Burton, M. M. Grimes, C. N. Powers, and M. H. Manjili. 2012. CD44(+)/CD24(-/low) cancer stem/progenitor cells are more abundant in triple-negative invasive breast carcinoma phenotype and are associated with poor outcome. *Hum. Pathol.* 43: 364-373.

8. Lorusso, G. and C. Ruegg. 2008. The tumor microenvironment and its contribution to tumor evolution toward metastasis. *Histochem. Cell Biol.* 130: 1091-1103.

9. Talmadge, J. E. and I. J. Fidler. 2010. AACR centennial series: the biology of cancer metastasis: historical perspective. *Cancer Res.* 70: 5649-5669.

10. Minn, A. J., G. P. Gupta, P. M. Siegel, P. D. Bos, W. Shu, D. D. Giri, A. Viale, A. B. Olshen, W. L. Gerald, and J. Massague. 2005. Genes that mediate breast cancer metastasis to lung. *Nature* 436: 518-524.

11. Valastyan, S. and R. A. Weinberg. 2011. Tumor metastasis: molecular insights and evolving paradigms. *Cell* 147: 275-292.

12. Mani, S. A., W. Guo, M. J. Liao, E. N. Eaton, A. Ayyanan, A. Y. Zhou, M. Brooks, F. Reinhard, C. C. Zhang, M. Shipitsin, L. L. Campbell, K. Polyak, C. Brisken, J. Yang, and R. A. Weinberg. 2008. The epithelial-mesenchymal transition generates cells with properties of stem cells. *Cell* 133: 704-715.

13. Morel, A. P., M. Lievre, C. Thomas, G. Hinkal, S. Ansieau, and A. Puisieux. 2008. Generation of breast cancer stem cells through epithelial-mesenchymal transition. *PLoS One* 3: e2888.

14. Al-Hajj, M., M. S. Wicha, A. Benito-Hernandez, S. J. Morrison, and M. F. Clarke. 2003. Prospective identification of tumorigenic breast cancer cells. *Proc. Natl. Acad. Sci. U. S. A.* 100: 3983-3988.

15. Al-Hajj, M., M. W. Becker, M. Wicha, I. Weissman, and M. F. Clarke. 2004. Therapeutic implications of cancer stem cells. *Curr. Opin. Genet. Dev.* 14: 43-47.

16. Phillips, T. M., W. H. McBride, and F. Pajonk. 2006. The response of CD24(-/low)/CD44+ breast cancer-initiating cells to radiation. *J. Natl. Cancer Inst.* 98: 1777-1785.

17. Dean, M., T. Fojo, and S. Bates. 2005. Tumour stem cells and drug resistance. *Nat. Rev. Cancer.* 5: 275-284.

18. Li, X., M. T. Lewis, J. Huang, C. Gutierrez, C. K. Osborne, M. F. Wu, S. G. Hilsenbeck, A. Pavlick, X. Zhang, G. C. Chamness, H. Wong, J. Rosen, and J. C. Chang. 2008. Intrinsic resistance of tumorigenic breast cancer cells to chemotherapy. *J. Natl. Cancer Inst.* 100: 672-679.

19. Lesley, J., R. Hyman, N. English, J. B. Catterall, and G. A. Turner. 1997. CD44 in inflammation and metastasis. *Glycoconj. J.* 14: 611-622.

20. Goodison, S., V. Urquidi, and D. Tarin. 1999. CD44 cell adhesion molecules. *Mol. Pathol.* 52: 189-196.

21. Lee, K. M., J. H. Ju, K. Jang, W. Yang, J. Y. Yi, D. Y. Noh, and I. Shin. 2012. CD24 regulates cell proliferation and transforming growth factor beta-induced epithelial to mesenchymal transition through modulation of integrin beta1 stability. *Cell. Signal.* 24: 2132-2142.

22. Cufi, S., A. Vazquez-Martin, C. Oliveras-Ferraros, B. Martin-Castillo, L. Vellon, and J. A. Menendez. 2011. Autophagy positively regulates the CD44(+) CD24(-/low) breast cancer stem-like phenotype. *Cell. Cycle* 10: 3871-3885.

23. Santisteban, M., J. M. Reiman, M. K. Asiedu, M. D. Behrens, A. Nassar, K. R. Kalli, P. Haluska, J. N. Ingle, L. C. Hartmann, M. H. Manjili, D. C. Radisky, S. Ferrone, and K. L. Knutson. 2009. Immune-induced epithelial to mesenchymal transition in vivo generates breast cancer stem cells. *Cancer Res*. 69: 2887-2895.

24. Xie, G., Q. Yao, Y. Liu, S. Du, A. Liu, Z. Guo, A. Sun, J. Ruan, L. Chen, C. Ye, and Y. Yuan. 2012. IL-6-induced epithelial-mesenchymal transition promotes the generation of breast cancer stem-like cells analogous to mammosphere cultures. *Int. J. Oncol*. 40: 1171-1179.

25. Schafer, M. and S. Werner. 2008. Cancer as an overhealing wound: an old hypothesis revisited. *Nat. Rev. Mol. Cell Biol*. 9: 628-638.

26. DeNardo, D. G. and L. M. Coussens. 2007. Inflammation and breast cancer. Balancing immune response: crosstalk between adaptive and innate immune cells during breast cancer progression. *Breast Cancer Res*. 9: 212.

27. Suzuki, M., E. S. Mose, V. Montel, and D. Tarin. 2006. Dormant cancer cells retrieved from metastasis-free organs regain tumorigenic and metastatic potency. *Am. J. Pathol*. 169: 673-681.

28. Meltzer, A. 1990. Dormancy and breast cancer. *J. Surg. Oncol*. 43: 181-188.

29. Chambers, A. F., A. C. Groom, and I. C. MacDonald. 2002. Dissemination and growth of cancer cells in metastatic sites. *Nat. Rev. Cancer*. 2: 563-572.

30. Incorvati, J. A., S. Shah, Y. Mu, and J. Lu. 2013. Targeted therapy for HER2 positive breast cancer. *J. Hematol. Oncol*. 6: 38.

31. Talmadge, J. E., R. K. Singh, I. J. Fidler, and A. Raz. 2007. Murine models to evaluate novel and conventional therapeutic strategies for cancer. *Am. J. Pathol*. 170: 793-804.

32. Fidler, I. J., D. M. Gersten, and C. W. Riggs. 1977. Relationship of host immune status to tumor cell arrest, distribution, and survival in experimental metastasis. *Cancer* 40: 46-55.

33. Restifo, N. P., M. E. Dudley, and S. A. Rosenberg. 2012. Adoptive immunotherapy for cancer: harnessing the T cell response. *Nat. Rev. Immunol*. 12: 269-281.

34. Rosenberg, S. A., J. C. Yang, R. M. Sherry, U. S. Kammula, M. S. Hughes, G. Q. Phan, D. E. Citrin, N. P. Restifo, P. F. Robbins, J. R. Wunderlich, K. E. Morton, C. M. Laurencot, S. M. Steinberg, D. E. White, and M. E. Dudley. 2011. Durable complete responses in heavily pretreated patients with metastatic melanoma using T-cell transfer immunotherapy. *Clin. Cancer Res*. 17: 4550-4557.

35. Bernhard, H., J. Neudorfer, K. Gebhard, H. Conrad, C. Hermann, J. Nahrig, F. Fend, W. Weber, D. H. Busch, and C. Peschel. 2008. Adoptive transfer of autologous, HER2-specific, cytotoxic T lymphocytes for the treatment of HER2-overexpressing breast cancer. *Cancer Immunol. Immunother*. 57: 271-280.

36. Schuetz, F., K. Ehlert, Y. Ge, A. Schneeweiss, J. Rom, N. Inzkirweli, C. Sohn, V. Schirrmacher, and P. Beckhove. 2009. Treatment of advanced metastasized breast cancer with bone marrow-derived tumour-reactive memory T cells: a pilot clinical study. *Cancer Immunol. Immunother*. 58: 887-900.

37. Domschke, C., Y. Ge, I. Bernhardt, S. Schott, S. Keim, S. Juenger, M. Bucur, L. Mayer, M. Blumenstein, J. Rom, J. Heil, C. Sohn, A. Schneeweiss, P. Beckhove, and F. Schuetz. 2013. Long-term survival after adoptive bone marrow T cell therapy of advanced metastasized breast cancer: follow-up analysis of a clinical pilot trial. *Cancer Immunol. Immunother*. 62: 1053-1060.

38. Sun, Z., L. Shi, H. Zhang, Y. Shao, Y. Wang, Y. Lin, X. Li, and C. Bai. 2011. Immune modulation and safety profile of adoptive immunotherapy using expanded autologous activated lymphocytes against advanced cancer. *Clin. Immunol*. 138: 23-32.

39. Kammertoens, T., T. Schuler, and T. Blankenstein. 2005. Immunotherapy: target the stroma to hit the tumor. *Trends Mol. Med*. 11: 225-231.

40. Biragyn, A. and D. L. Longo. 2012. Neoplastic "Black Ops": cancer's subversive tactics in overcoming host defenses. *Semin. Cancer Biol*. 22: 50-59.

41. Liao, D., Y. Luo, D. Markowitz, R. Xiang, and R. A. Reisfeld. 2009. Cancer associated fibroblasts promote tumor growth and metastasis by modulating the tumor immune microenvironment in a 4T1 murine breast cancer model. *PLoS One* 4: e7965.

42. Olkhanud, P. B., D. Baatar, M. Bodogai, F. Hakim, R. Gress, R. L. Anderson, J. Deng, M. Xu, S. Briest, and A. Biragyn. 2009. Breast cancer lung metastasis requires expression of chemokine receptor CCR4 and regulatory T cells. *Cancer Res*. 69: 5996-6004.

43. Abe, F., A. J. Dafferner, M. Donkor, S. N. Westphal, E. M. Scholar, J. C. Solheim, R. K. Singh, T. A. Hoke, and J. E. Talmadge. 2010. Myeloid-derived suppressor cells in mammary tumor progression in FVB Neu transgenic mice. *Cancer Immunol. Immunother*. 59: 47-62.

44. Yu, J., W. Du, F. Yan, Y. Wang, H. Li, S. Cao, W. Yu, C. Shen, J. Liu, and X. Ren. 2013. Myeloid-derived suppressor cells suppress antitumor immune responses through IDO expression and correlate with lymph node metastasis in patients with breast cancer. *J. Immunol*. 190: 3783-3797.

45. Morales, J. K., M. Kmieciak, L. Graham, M. Feldmesser, H. D. Bear, and M. H. Manjili. 2009. Adoptive transfer of HER2/neu-specific T cells expanded with alternating gamma chain cytokines mediate tumor regression when combined with the depletion of myeloid-derived suppressor cells. *Cancer Immunol. Immunother*. 58: 941-953.

46. Kmieciak, M., D. Basu, K. K. Payne, A. Toor, A. Yacoub, X. Y. Wang, L. Smith, H. D. Bear, and M. H. Manjili. 2011. Activated NKT cells and NK cells render T cells resistant to myeloid-derived suppressor cells and result in an effective adoptive cellular therapy against breast cancer in the FVBN202 transgenic mouse. *J. Immunol*. 187: 708-717.

47. Chandra, D., A. Jahangir, W. Quispe-Tintaya, M. H. Einstein, and C. Gravekamp. 2013. Myeloid-derived suppressor cells have a central role in attenuated Listeria monocytogenes-based immunotherapy against metastatic breast cancer in young and old mice. *Br. J. Cancer* 108: 2281-2290.

48. Morales, J. K., M. Kmieciak, K. L. Knutson, H. D. Bear, and M. H. Manjili. 2010. GM-CSF is one of the main breast tumor-derived soluble factors involved in the differentiation of CD11b-Gr1- bone marrow progenitor cells into myeloid-derived suppressor cells. *Breast Cancer Res. Treat.* 123: 39-49.

49. Tuttle, T. M., T. H. Inge, K. P. Bethke, C. W. McCrady, G. R. Pettit, and H. D. Bear. 1992. Activation and growth of murine tumor-specific T-cells which have in vivo activity with bryostatin 1. *Cancer Res.* 52: 548-553.

50. Kazanietz, M. G., N. E. Lewin, F. Gao, G. R. Pettit, and P. M. Blumberg. 1994. Binding of [26-3H]bryostatin 1 and analogs to calcium-dependent and calcium-independent protein kinase C isozymes. *Mol. Pharmacol.* 46: 374-379.

51. Chatila, T., L. Silverman, R. Miller, and R. Geha. 1989. Mechanisms of T cell activation by the calcium ionophore ionomycin. *J. Immunol.* 143: 1283-1289.

52. Truneh, A., F. Albert, P. Golstein, and A. M. Schmitt-Verhulst. 1985. Early steps of lymphocyte activation bypassed by synergy between calcium ionophores and phorbol ester. *Nature* 313: 318-320.

53. Kmieciak, M., K. L. Knutson, C. I. Dumur, and M. H. Manjili. 2007. HER-2/neu antigen loss and relapse of mammary carcinoma are actively induced by T cell-mediated anti-tumor immune responses. *Eur. J. Immunol.* 37: 675-685.

54. Kmieciak, M., J. K. Morales, J. Morales, E. Bolesta, M. Grimes, and M. H. Manjili. 2008. Danger signals and nonself entity of tumor antigen are both required for eliciting effective immune responses against HER-2/neu positive mammary carcinoma: implications for vaccine design. *Cancer Immunol. Immunother.* 57: 1391-1398.

55. Disis, M. L., V. Goodell, K. Schiffman, and K. L. Knutson. 2004. Humoral epitope-spreading following immunization with a HER-2/neu peptide based vaccine in cancer patients. *J. Clin. Immunol.* 24: 571-578.

56. Disis, M. L., D. R. Wallace, T. A. Gooley, Y. Dang, M. Slota, H. Lu, A. L. Coveler, J. S. Childs, D. M. Higgins, P. A. Fintak, C. dela Rosa, K. Tietje, J. Link, J. Waisman, and L. G. Salazar. 2009. Concurrent trastuzumab and HER2/neu-specific vaccination in patients with metastatic breast cancer. *J. Clin. Oncol.* 27: 4685-4692.

57. Guy, C. T., M. A. Webster, M. Schaller, T. J. Parsons, R. D. Cardiff, and W. J. Muller. 1992. Expression of the neu protooncogene in the mammary epithelium of transgenic mice induces metastatic disease. *Proc. Natl. Acad. Sci. U. S. A.* 89: 10578-10582.

58. Kmieciak, M., M. Gowda, L. Graham, K. Godder, H. D. Bear, F. M. Marincola, and M. H. Manjili. 2009. Human T cells express CD25 and Foxp3 upon activation and exhibit effector/memory phenotypes without any regulatory/suppressor function. *J. Transl. Med.* 7: 89-5876-7-89.

59. Manjili, M. H., H. Arnouk, K. L. Knutson, M. Kmieciak, M. L. Disis, J. R. Subjeck, and A. L. Kazim. 2006. Emergence of immune escape variant of mammary tumors that has distinct proteomic profile and a reduced ability to induce "danger signals". *Breast Cancer Res. Treat.* 96: 233-241.

60. Campbell, M. J., W. S. Wollish, M. Lobo, and L. J. Esserman. 2002. Epithelial and fibroblast cell lines derived from a spontaneous mammary carcinoma in a MMTV/neu transgenic mouse. *In Vitro Cell. Dev. Biol. Anim.* 38: 326-333.

61. Rizki, A., V. M. Weaver, S. Y. Lee, G. I. Rozenberg, K. Chin, C. A. Myers, J. L. Bascom, J. D. Mott, J. R. Semeiks, L. R. Grate, I. S. Mian, A. D. Borowsky, R. A. Jensen, M. O. Idowu, F. Chen, D. J. Chen, O. W. Petersen, J. W. Gray, and M. J. Bissell. 2008. A human breast cell model of preinvasive to invasive transition. *Cancer Res.* 68: 1378-1387.

62. Spano, D., C. Heck, P. De Antonellis, G. Christofori, and M. Zollo. 2012. Molecular networks that regulate cancer metastasis. *Semin. Cancer Biol.* 22: 234-249.

63. Lim, E., D. Wu, B. Pal, T. Bouras, M. L. Asselin-Labat, F. Vaillant, H. Yagita, G. J. Lindeman, G. K. Smyth, and J. E. Visvader. 2010. Transcriptome analyses of mouse and human mammary cell subpopulations reveal multiple conserved genes and pathways. *Breast Cancer Res.* 12: R21.

64. Prat, A., J. S. Parker, O. Karginova, C. Fan, C. Livasy, J. I. Herschkowitz, X. He, and C. M. Perou. 2010. Phenotypic and molecular characterization of the claudin-low intrinsic subtype of breast cancer. *Breast Cancer Res.* 12: R68.

65. Blick, T., E. Widodo, H. Hugo, M. Waltham, M. E. Lenburg, R. M. Neve, and E. W. Thompson. 2008. Epithelial mesenchymal transition traits in human breast cancer cell lines. *Clin. Exp. Metastasis* 25: 629-642.

66. Blick, T., H. Hugo, E. Widodo, M. Waltham, C. Pinto, S. A. Mani, R. A. Weinberg, R. M. Neve, M. E. Lenburg, and E. W. Thompson. 2010. Epithelial mesenchymal transition traits in human breast cancer cell lines parallel the CD44(hi/)CD24 (lo/-) stem cell phenotype in human breast cancer. *J. Mammary Gland Biol. Neoplasia* 15: 235-252.

67. Evdokimova, V., C. Tognon, T. Ng, P. Ruzanov, N. Melnyk, D. Fink, A. Sorokin, L. P. Ovchinnikov, E. Davicioni, T. J. Triche, and P. H. Sorensen. 2009. Translational activation of snail1 and other developmentally regulated transcription factors by YB-1 promotes an epithelial-mesenchymal transition. *Cancer. Cell.* 15: 402-415.

68. To, K., A. Fotovati, K. M. Reipas, J. H. Law, K. Hu, J. Wang, A. Astanehe, A. H. Davies, L. Lee, A. L. Stratford, A. Raouf, P. Johnson, I. M. Berquin, H. D. Royer, C. J. Eaves, and S. E. Dunn. 2010. Y-box binding protein-1 induces the expression of CD44 and CD49f leading to enhanced self-renewal, mammosphere growth, and drug resistance. *Cancer Res.* 70: 2840-2851.

69. Yu, M., G. A. Smolen, J. Zhang, B. Wittner, B. J. Schott, E. Brachtel, S. Ramaswamy, S. Maheswaran, and D. A. Haber. 2009. A developmentally regulated inducer of EMT, LBX1, contributes to breast cancer progression. *Genes Dev*. 23: 1737-1742.

70. Wyckoff, J. B., Y. Wang, E. Y. Lin, J. F. Li, S. Goswami, E. R. Stanley, J. E. Segall, J. W. Pollard, and J. Condeelis. 2007. Direct visualization of macrophage-assisted tumor cell intravasation in mammary tumors. *Cancer Res*. 67: 2649-2656.

71. Hiratsuka, S., K. Nakamura, S. Iwai, M. Murakami, T. Itoh, H. Kijima, J. M. Shipley, R. M. Senior, and M. Shibuya. 2002. MMP9 induction by vascular endothelial growth factor receptor-1 is involved in lung-specific metastasis. *Cancer. Cell*. 2: 289-300.

72. Ting, A. H., K. M. McGarvey, and S. B. Baylin. 2006. The cancer epigenome--components and functional correlates. *Genes Dev*. 20: 3215-3231.

73. Zeng, S., Y. Yang, Y. Tan, C. Lu, Y. Pan, L. Chen, and G. Lu. 2012. ERBB2-induced inflammation in lung carcinogenesis. *Mol. Biol. Rep*. 39: 7911-7917.

74. Ghajar, C. M., H. Peinado, H. Mori, I. R. Matei, K. J. Evason, H. Brazier, D. Almeida, A. Koller, K. A. Hajjar, D. Y. Stainier, E. I. Chen, D. Lyden, and M. J. Bissell. 2013. The perivascular niche regulates breast tumour dormancy. *Nat. Cell Biol*. 15: 807-817.

75. Acuff, H. B., K. J. Carter, B. Fingleton, D. L. Gorden, and L. M. Matrisian. 2006. Matrix metalloproteinase-9 from bone marrow-derived cells contributes to survival but not growth of tumor cells in the lung microenvironment. *Cancer Res*. 66: 259-266.

76. DuPre', S. A. and K. W. Hunter Jr. 2007. Murine mammary carcinoma 4T1 induces a leukemoid reaction with splenomegaly: association with tumor-derived growth factors. *Exp. Mol. Pathol*. 82: 12-24.

77. Nagaraj, S. and D. I. Gabrilovich. 2008. Tumor escape mechanism governed by myeloid-derived suppressor cells. *Cancer Res*. 68: 2561-2563.

78. Morse, M. A., H. K. Lyerly, T. M. Clay, O. Abdel-Wahab, S. Y. Chui, J. Garst, J. Gollob, P. M. Grossi, M. Kalady, P. J. Mosca, M. Onaitis, J. H. Sampson, H. F. Seigler, E. M. Toloza, D. Tyler, J. Vieweg, and Y. Yang. 2004. Immunotherapy of surgical malignancies. *Curr. Probl. Surg*. 41: 15-132.

79. Sallusto, F., D. Lenig, R. Forster, M. Lipp, and A. Lanzavecchia. 1999. Two subsets of memory T lymphocytes with distinct homing potentials and effector functions. *Nature* 401: 708-712.

80. Klebanoff, C. A., L. Gattinoni, and N. P. Restifo. 2006. CD8+ T-cell memory in tumor immunology and immunotherapy. *Immunol. Rev*. 211: 214-224.

81. Klebanoff, C. A., L. Gattinoni, and N. P. Restifo. 2012. Sorting through subsets: which T-cell populations mediate highly effective adoptive immunotherapy? *J. Immunother*. 35: 651-660.

82. Bennett, M. W., J. O'Connell, G. C. O'Sullivan, C. Brady, D. Roche, J. K. Collins, and F. Shanahan. 1998. The Fas counterattack in vivo: apoptotic depletion of tumor-infiltrating lymphocytes associated with Fas ligand expression by human esophageal carcinoma. *J. Immunol.* 160: 5669-5675.

83. Franco, E. L. and D. M. Harper. 2005. Vaccination against human papillomavirus infection: a new paradigm in cervical cancer control. *Vaccine* 23: 2388-2394.

84. Seong, S. Y. and P. Matzinger. 2004. Hydrophobicity: an ancient damage-associated molecular pattern that initiates innate immune responses. *Nat. Rev. Immunol.* 4: 469-478.

85. Levine, B. L. and C. H. June. 2013. Perspective: assembly line immunotherapy. *Nature* 498: S17.

86. Kumar, A. J., E. O. Hexner, N. V. Frey, S. M. Luger, A. W. Loren, R. Reshef, J. Boyer, J. Smith, E. A. Stadtmauer, B. L. Levine, C. H. June, D. L. Porter, and S. C. Goldstein. 2013. Pilot study of prophylactic ex vivo costimulated donor leukocyte infusion after reduced-intensity conditioned allogeneic stem cell transplantation. *Biol. Blood Marrow Transplant.* 19: 1094-1101.

87. Kleeberg, U. R., M. Fink, H. W. Tessen, A. Nennecke, S. Hentschel, and S. Bartels. 2013. Adjuvant therapy reduces the benefit of palliative treatment in disseminated breast cancer - own findings and review of the literature. *Onkologie* 36: 348-356.

88. Gennari, A., P. Conte, R. Rosso, C. Orlandini, and P. Bruzzi. 2005. Survival of metastatic breast carcinoma patients over a 20-year period: a retrospective analysis based on individual patient data from six consecutive studies. *Cancer* 104: 1742-1750.

89. Gennari, A., M. Stockler, M. Puntoni, M. Sormani, O. Nanni, D. Amadori, N. Wilcken, M. D'Amico, A. DeCensi, and P. Bruzzi. 2011. Duration of chemotherapy for metastatic breast cancer: a systematic review and meta-analysis of randomized clinical trials. *J. Clin. Oncol.* 29: 2144-2149.

90. Brent, L., I. R. Cohen, P. C. Doherty, M. Feldmann, P. Matzinger, L. Ghost, S. T. Holgate, P. Lachmann, N. A. Mitchison, G. Nossal, N. R. Rose, and R. Zinkernagel. 2007. Crystal-ball gazing--the future of immunological research viewed from the cutting edge. *Clin. Exp. Immunol.* 147: 1-10.

91. Velasco-Velazquez, M. A., V. M. Popov, M. P. Lisanti, and R. G. Pestell. 2011. The role of breast cancer stem cells in metastasis and therapeutic implications. *Am. J. Pathol.* 179: 2-11.

Vita

Charles Edward Hall was born on March 15, 1985, in Fredericksburg, Virginia, and is an American citizen. He attended Chancellor High School, Spotsylvania, Virginia graduating in 2003. He received a Bachelor of Science in Biology and a Bachelor of Music in Music Industry from James Madison University, Harrisonburg, Virginia in 2008. He started work in the fall of 2009 at the American Type Culture Collection (ATCC), Manassas, Virginia for over a year as an Associate Biologist prior to enrollment at VCU in the Graduate School in the fall of 2011.